Methodology for Transient Stability Analysis of an Interconnected Power Grid from a Reduced Order System Model

A Thesis
Presented in Partial Fulfillment of the Requirements for the
Degree of Master of Science
with a
Major in Electrical Engineering
in the
College of Graduate Studies
University of Idaho
by
James G O'Brien

Major Professor:	Brian K. Johnson, Ph.D., P.E.
Committee Members:	Herbert Hess, Ph.D.
	Yacine Chakhchoukh, Ph.D.
Department Administrator:	Joseph Law, Ph.D.

December 2020

Authorization to Submit Thesis

This thesis of James G O'Brien, submitted for the degree of Master of Science with a Major in Electrical Engineering and titled "Methodology for Transient Stability Analysis of an Interconnected Power Grid from a Reduced Order System Model," has been reviewed in final form. Permission, as indicated by the signatures and dates below, is now granted to submit final copies to the College of Graduate Studies for approval.

Major Professor:	_____ Brian K. Johnson, Ph.D., P.E.	Date: _____
Committee Members:	_____ Herbert Hess, Ph.D.	Date: _____
	_____ Yacine Chakhchoukh, Ph.D.	Date: _____
Department Administrator:	_____ Joseph Law, Ph.D.	Date: _____

Abstract

Today, the power system of the Baltic States (comprised of Lithuania, Latvia, and Estonia) is synchronized with the Integrated/Unified Power System (IPS/UPS) of Russia and Belarus. It is planned that by 2025 they desynchronize from the IPS/UPS system and to join the largest interconnection in the world, Continental Europe. The goal of this master thesis is to delve further into planned out-year operations in the European power grid with the synchronized connection of the Baltic States. To understand this topology, there needs to be a methodology for performing the power system analyses of the interconnected large power grid, particularly the case when the smaller grid is being connected to a large power system and when the models available are limited in terms of fidelity and completeness.

The focus of this research is threefold: 1) develop a procedure on how to find an AC solution from an approximated DC solution; 2) present a methodology for building the transmission system model from scratch using only publicly available data and 3) conduct dynamic studies to ensure reliable operation of the interconnected system. In this research, an open-source European grid model will be used, however, the available model was only built to study simple DC power flow solutions. The process of finding an AC solution from a DC one has been a difficult topic for the power system industry, and a new methodology on how to achieve this is proposed and will be discussed and demonstrated. The Baltic States transmission power grid equivalent will be added by using publicly available data for the transmission system topology, generation capacity, and load distribution. Finally, dynamic generation machine and control models are going to be introduced and assigned to the model, based upon the type of generation that exists at each location (or large-scale equivalent).

The built model of the integrated grid will allow a wide range of studies, from steady state to dynamic and it will help in the development of the new control and protection schemes to assist in increased system stability. To demonstrate the value of the developed model, a transient stability analysis will be performed on the interconnected model to analyze both the impact of the Baltic States on the dynamic stability of the interconnected grid, and the impact of events in the European grid on the Baltic States through the synchronous connection.

Acknowledgements

First, I would like to express my sincere gratitude and respect to my advisor, Dr. Brian K. Johnson, for his guidance and support throughout the course of this research. I also wish to thank my committee members, Dr. Herbert Hess, and Dr. Yacine Chakhchoukh, for their suggestions, time, and support.

I want to express my appreciation to Pacific Northwest National Laboratories (PNNL) for the provided assistance necessary to complete this degree.

Special thanks to Giedrius Radvila from Litgrid (Lithuania grid operator) and Michael White from PNNL for all the informative discussions and interactions, which have been extremely valuable for my research.

Thanks also go to my friends, and colleagues for their help and support throughout my graduate study.

Finally, I wish to thank my family for their unconditional love, encouragement, and patience.

Dedication

I want to make a special dedication to my grandfather, Jim Grant. While he is not here to see me finish my degree, his support and encouragement throughout the years was a constant source of inspiration. The guidance, advice, and wisdom he shared will be something that I will keep throughout the rest of my life. Thanks Popeye.

Table of Contents

List of Tables

List of Figures

Chapter 1: Introduction

1.1. Motivation and Overview

In a power system based on traditional architecture, most of the electric power is generated with bulk generators remotely located from consumers, and it is delivered to users through a transmission and distribution system. Electricity is typically produced at lower voltage levels and then using the transformers “stepped-up” for long-distance transportation over the transmission grid. The transmission system is made up of high voltage equipment that transfers electricity from one location to another, where transmission lines are interconnected forming the mesh topology. These high voltages enable more power to be transferred at a lower current, thereby decreasing the overall heating losses (I^2*R). Close to load centers, electricity is “stepped-down” and power is delivered throughout distribution systems that operate at a lower voltage and typically form a radial topology.

Operating a high voltage interconnected system provides both reliability and economic benefits by forming the stronger system that is less susceptible to major disturbances and allows for the operation of electrical markets so that power can be bought, sold, and traded across the wide regions [1]. The United States power grid is comprised of three alternating current (AC) power grids, also called “interconnections”: The Eastern Interconnection (EI), Western Interconnection (WECC), and the Texas Interconnection (ERCOT). All utilities within the footprint of the interconnections are electrically tied together during the normal system operation and operate at a synchronized frequency regulated tightly close to 60 Hz. Similarly, the power system in Europe is divided into five synchronous areas, namely Continental Europe (CE), Northern Europe (NE), Baltic Integrated Power System, Great Britain (GB), and Ireland-Northern Ireland (IRE), all of which are operating at the nominal frequency of 50Hz and are electrically connected through high-voltage direct current links (HVDC).

Today, the power system of the Baltic States which includes Lithuania, Latvia, and Estonia, is synchronized with the Integrated/Unified Power System (IPS/UPS) of Russia and Belarus forming the BRELL (Belarus, Russia, Estonia, Latvia, and Lithuania) ring [2]. Within the BRELL ring, the Russian power system provides frequency regulation and ensures a secure system operation. Even though Baltic states already participate in the European Market and trading the electricity, for various reasons (e.g., political, economic, to name a few), it is planned that by 2025 they desynchronize from the IPS/UPS system and to join the largest interconnection in the world, Continental Europe. Since the decision was made, multiple feasibility studies have been conducted and it has been concluded

and approved that the Baltic States will be synchronized to CE through an HVAC Lithuania-Poland interconnector, including the “soft-coupling” through existing HVDC links [3].

The proposed synchronization infrastructure through one HVAC link resembles the topology seen between Canadian province-Alberta and WECC. Alberta has an electrical interconnection with British Columbia (BC) via a single 500 kV AC transmission circuit in parallel with two 138 kV lines. In 2013, a new 230 kV AC line was commissioned between Alberta and Montana to strengthen system reliability and add market capability [4]. Even with the additional line, the impact of the “weak” connection between Alberta and WECC is still very strong in terms of the dynamic stability of the system. The two most spread oscillatory modes present in WECC are North-South Mode A (NSA) nominally near 0.2 Hz and North-South Mode B (NSB) nominally near 0.4 Hz, and are mostly affected by the system topology, particularly by the connection of the Alberta to the rest of the system [5]. It has been observed that once Alberta separates from the rest of the system, the two beforementioned modes merge in one newly formed mode. To keep the lights on, and ensure the reliability and stability of the interconnection, a key strategy was to improve and validate the system models, which in return enabled the accurate studies, monitoring, and problem mitigation.

With the upcoming desynchronization project, the Baltic States are facing a similar predicament in the near future and a good system model is mandatory to be able to adequately prepare for the upcoming changes. Since the 2000s mostly feasibility studies are carried out using simplified system models (network models for load flow calculations, models populated with the incomplete regional and wide are stability data, and market models). In order to successfully join the CE, Baltic States planners will need to perform numerous additional system studies, ranging from planning and expansion (load flow), as well as more advanced dynamic analysis to designed and implement new control and protection schemes. To be able to accurately characterize the system behavior and design the control schemes, an AC network model that includes dynamics information from the Baltic States, as well as CE grid, will need to be implemented.

The aim of this thesis is to develop an integrated transmission network model of the CE and Baltic States from the publicly available data that will allow one to carry out a wide range of power system studies from steady-state power flow to a transient and small signal stability analysis. Through the resources provided by the European Network of Transmission System Operators (ENTSO-E) a transmission system network model can be obtained. However, the given model only has a DC solution, and to be adequate for the advanced system studies it needs to be modified to find an AC solution as well as populated with the dynamic data for the transient stability analyses.

Finding an AC solution from a DC solution is not a trivial task and there are no dedicated methodologies on how one can do that. A DC solution is only concerned with the MW flows, and MVars are neglected, thus stability studies, such as transient and voltage cannot be carried. To generate the model adequate for the transient stability analysis, this research will develop a methodology to fill the missing data and a procedure for the recovering AC solution from a DC one. An approach to strengthen this network and also generate dynamic data for the case from publicly available data sources will be explored.

1.2. Thesis Organization

The rest of this thesis is organized as follows. Chapter 2 describes the basics of power system modeling and analysis. In Chapter 3 the proposed procedure for the recovery of AC solution from a DC case is presented. Chapter 4 deals with the building of the Baltic States transmission system from the publicly available information and its connection to a larger grid. After the integration, a step by step iterative framework is applied to a combined CE with the Baltic States to find an AC solution. The procedure on building the dynamic model is discussed in Chapter 5 and applied to developed integrated power networks. Chapter 5 also shows the impact of system interconnection on the dynamic behavior of the overall grid through modal analysis. Mode frequency and damping ratios of the CE grid before and after the Baltic States connection are being analyzed and results are presented. Conclusions are given in Chapter 6 as well as the suggestions for future research. System data are given in the Appendix.

Chapter 2: Power System Modeling and Analysis

2.1. Introduction

A power system is a highly complex large-scale network of interconnected components. The main elements of the power system are generators, transmission and distribution systems, and loads. Transmission and distribution networks consist of transformers, lines, capacitors, reactors, and protection devices and are responsible to transmit power over a wide region from generation stations to customers (consumers) at different voltage levels. The basic structure of the electric power system is given in Figure 1. The transmission system forms the backbone of the integrated power system and operates at the highest voltage levels (above 130 kV), whereas the distribution system operates at the lower voltage levels (<69kV).

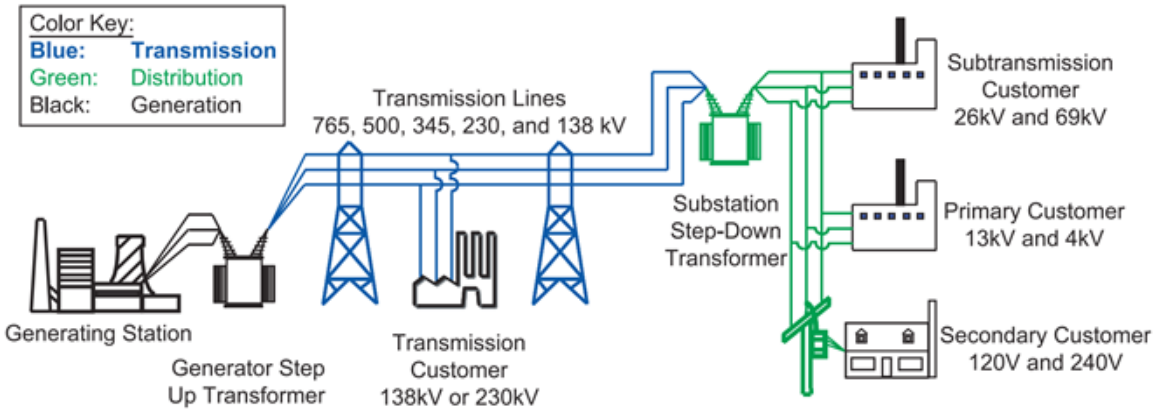

Figure 1. The basic structure of the power system [6]

Simulations of the physical prototype have been a common practice for studying the behavior of the grid, for real-time operation as well as for planning. The general approach for studying any physical system is depicted in Figure 2. A model of a system allows investigation and prediction of the system behavior; however, the prediction highly depends on the realism of the model. In other words, the value of simulation is dependent on how well the model represents the real system regarding the questions that need to be answered.

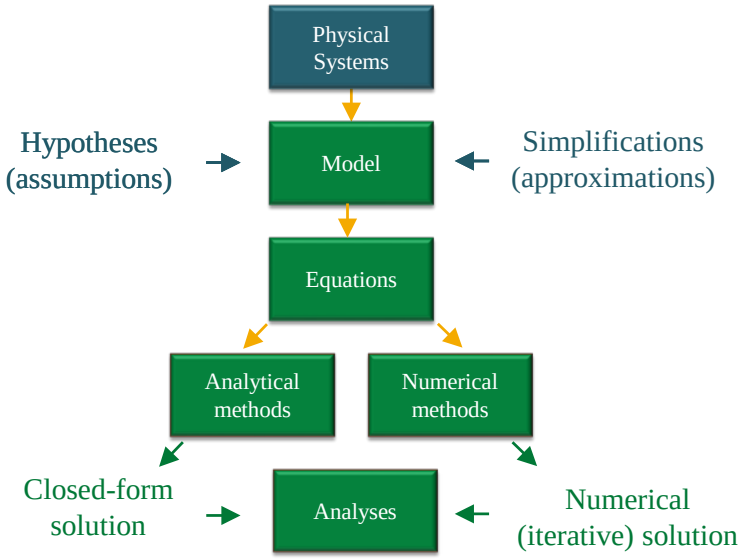

Figure 2. A general approach for studying physical systems

Performing power system analysis is the understanding of the behavior of the power system network as a whole. The key analysis question in choosing the appropriate model is to determine the time frame of interest. Different power system components have different time scales of response and depending upon the analysis type each component might have a different model approximation.

In general, the system can be analyzed either under steady-state or under dynamic or transient conditions during and after disturbances. Figure 3 shows various types of power system analysis and the timeframes of interest. Even though the real system is always changing, over a time period of interest, this system can be approximated as an unchanging system. Thus, for the steady-state analysis, the power system state is assumed as unchanging (quasi-steady-state). The primary steady-state analysis tool is the power flow. This type of system study is used for both, offline and online analysis. Models employed in this type of studies assume loads with constant power, current or impedance, approximate governor response, etc.

On the other side, the dynamic-type analysis looks at how the power system responds over time when it has been perturbed and moved away from the equilibrium point, and the models are developed with more details to better mimic dynamic behavior of the component.

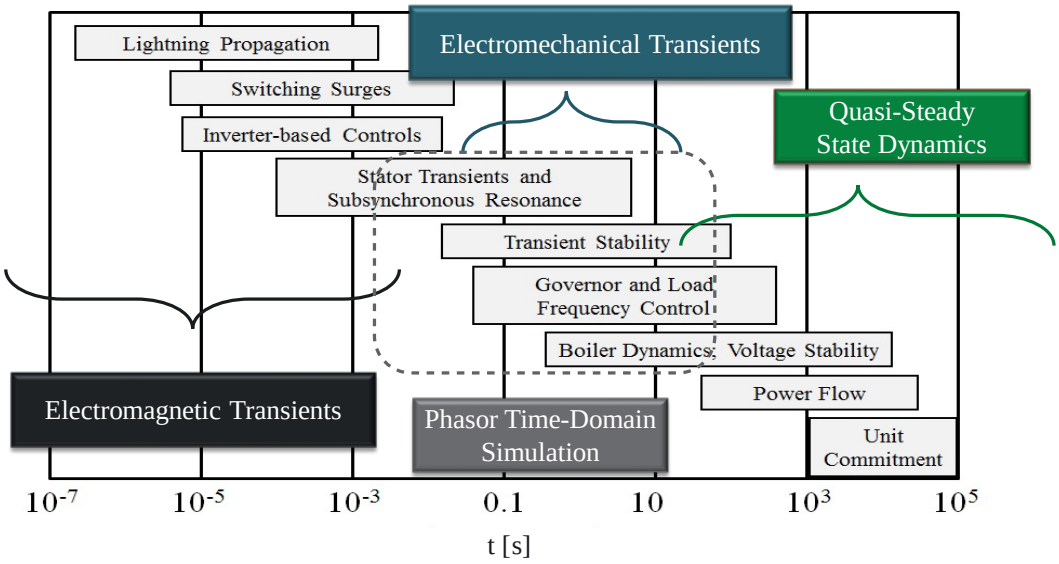

Figure 3. Time scales in power system [7]

2.2. Modeling of the Components and Input Data

The model of the power system is built by modeling the individual system components and defining the relationship between them in terms of equations. To be able to simulate the power system, each component needs to be represented by its model. Component models are mathematical representations of components, usually by parameters within equations. When choosing the appropriate model, it is important to distinguish between model fidelity and parameter accuracy.

Large-scale electrical systems are almost exclusively three-phase. Common analysis tools such as power flow and transient stability often assume balanced operation and are positive sequence, whereas electromagnetic transients tools (commonly known as electromagnetic transients programs EMTP) consider the full three-phase models in the time domain. For the protection analysis, three-phase phasor-based models are required in order to calculate the settings for the unbalanced faults. Since the distribution systems are often unbalanced, full three-phase models are also used.

A decision on the model choice should be made based on the phenomenon that is being studied and the knowledge of the actual system composition. In this thesis, the focus is on building the model for the power flow and transient stability studies of a large power grid, thus, the presented models are for balanced positive sequence studies.

2.2.1. Generator

Generators convert primary energy into electrical energy. Primary energy can come from coal, gas, fuel, nuclear reactor, or from a renewable resource such as wind, solar, hydro. Today the majority of

the electricity is still produced by conventional generation sources that use synchronous machines. Depending on the type of the studies (steady or dynamic) two different models will be used.

Steady-state model

For power flow studies generator can be modeled as a constant power source that is operating at a fixed terminal voltage [1]. The equivalent circuit is depicted in Figure 4 where E_f is internally generated voltage, r_a represents the resistance in the stator windings, Xs is synchronous reactance (effective coupled stator reactance), and V_T is a terminal voltage. These parameters can be determined through open-circuit and short-circuit tests.

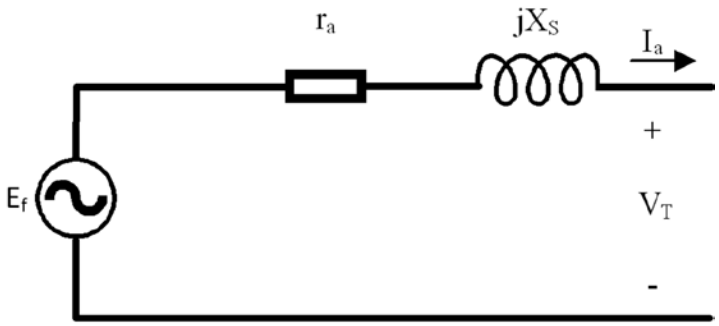

Figure 4. Generator equivalent circuit

Dynamic model

For transient stability studies, however, generators need to be represented with higher fidelity models. Usually, some of the standard/classical machine models (e.g., GENSAL or GENROU [10]) are used along with the automatic control systems including the excitation system, governor, and stabilizer as depicted in Figure 5.

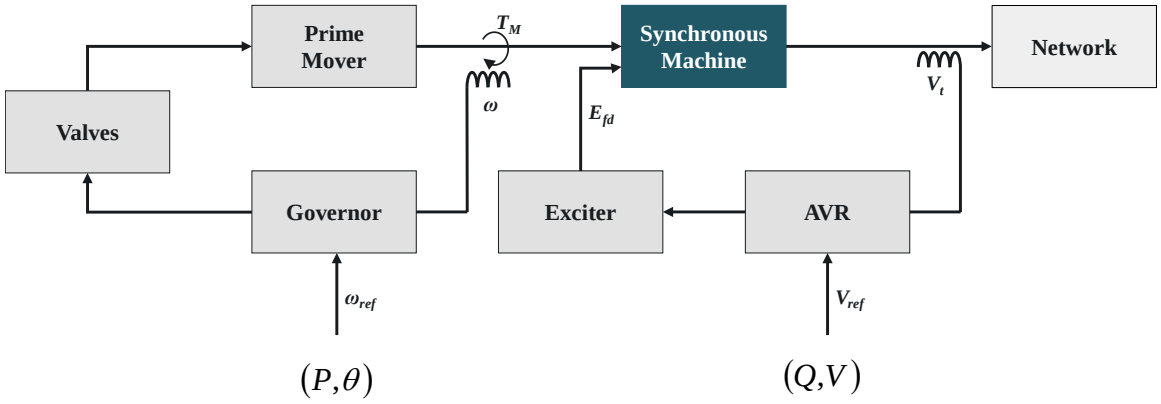

Figure 5. Generator model for dynamic studies

Key simulation parameters that describe the machine model are given in Table 1. For the purpose of the simulation in this thesis, a set of typical (default) values will be used. The machine models also include the prime mover and connecting shaft that drive the synchronous generator.

Table 1. Synchronous machine simulation parameters

Parameter	**Description**
R_s	Stator Resistance
X_l	Stator Leakage
X_d, X_q	Synchronous Reactance
X'_d, X'_q	Transient Reactance
X''_d, X''_q	Sub-Transient Reactance
T'_{d0}, T'_{q0}	Open Circuit Transient Time Const.
T''_{d0}, T''_{q0}	Open Circuit Sub-Transient Time Const.
S1	Saturation Factor at 1.0 pu flux
S12	Saturation Factor at 1.2 pu flux
Rcom	Compensation Resistance for Voltage Control
Xcom	Compensation Reactance for Voltage Control
H	Inertia Constant (s)
D	Damping Factor

Governing systems are used to regulate the frequency by controlling the prime mover's mechanical power output, and as in the case with the machine models, some standardized classical models will be used (e.g., HYGOV [10]). These models take into consideration not only the time that takes for valves to reposition to allow more fuel to enter, but also how long it takes for this fuel to accelerate to provide the increased demand.

The function of the excitation system is twofold:1) to provide direct current to the synchronous generator field winding and to perform control and 2) protective functions, among which are control of reactive power flow through means of terminal voltage control. In order to maintain the terminal voltage, the generator needs to vary its reactive power output (higher voltages require more reactive power).

Finally, power system stabilizers are used to dampen system oscillations through excitation control by modulating the generator field voltage, thereby indirectly affecting the generator power output. This is done by modifying the voltage setpoint (as depicted in Figure 6) to be out of phase with the natural oscillations. In this method the power output of the generation unit changes, working against the oscillation itself, thereby increasing damping.

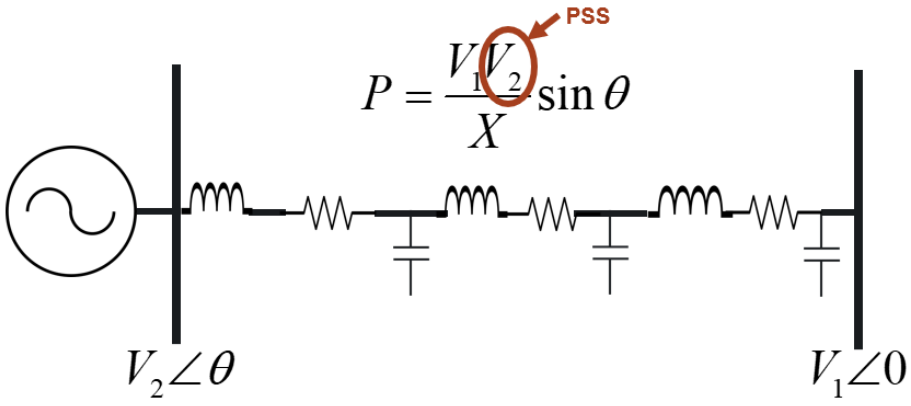

Figure 6 PSS impacting the real power output

2.2.2. Transformer

Power transformers transform AC voltage and current to optimum levels for generation, transmission, distribution, and utilization of electric power. The transformer consists of two sets of windings (sometimes three) that are coupled magnetically. Transformers in which the windings are also coupled electrically are called autotransformers. Figure 7 shows the simplified equivalent circuit of a real transformer and it includes losses, leakage flux, and has a finite permeability of the magnetic core. Very often shunt elements are assumed to have a high impedance and are neglected. Parameter "a" is a turns ratio and it is equal to the number of primary turns divided by the number of turns of the secondary coil. The turns ratio provides the unloaded operation of the transformer, however in reality the voltage and current ratio may not be equal to the physical ratio due to the real and reactive power losses. The parameters of the model can be acquired through the open circuit and short circuit tests and from the nameplate data.

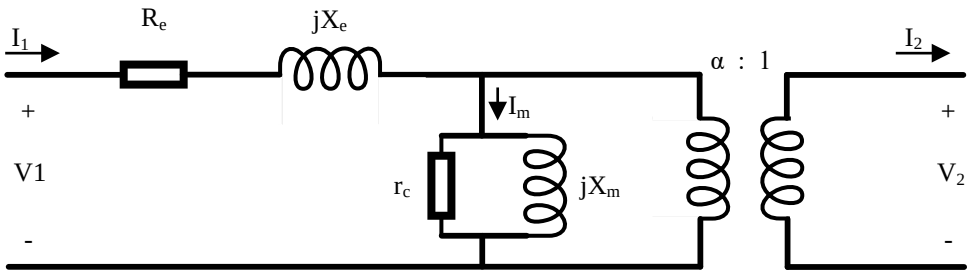

Figure 7. Simplified transformer equivalent circuit

If the transformer has a fixed turns ratio and the shunt branches are neglected, then transformers models are similar to a short transmission line. There are configurations where the tap ratio is variable, and those transformers are called Load Tap-Changing transformers (LTC). The tap ratio can be changed by changing the number of turns coupled in a winding using a tap changer. Those are used to regulate bus voltage. Further, a group of the transformers that are used to control the phase angle across the transformers are called phase shifting transformers or Phase Angle Regulators (PARs). They are used to control the power flow through the transformer and to prevent line overloads. The models of the two classes of transformers include shunt elements related to the tap setting or phase shift set point when implemented in phasor-based solutions.

2.2.3. Transmission Line

Transmission lines are the most common method used to transfer electric power over long distances and are usually three-phase AC overhead lines. Three-phase AC underground and undersea cables are used as well. With the technology improvements in the late 20th-century high-voltage direct-current (HVDC) lines are also being used for power transfer more frequently. Even though the losses associated with the power transfer over HVDC are lower than AC of the same capacity over larger distances, due to the inherent cost of building the HVDC station, AC lines are still the primary way of transferring the electrical power in areas where overhead lines are used. Figure 8 shows an approximated comparison between overhead HVAC and HVDC links in terms of losses Fig (a) and in terms of cost Fig (b).

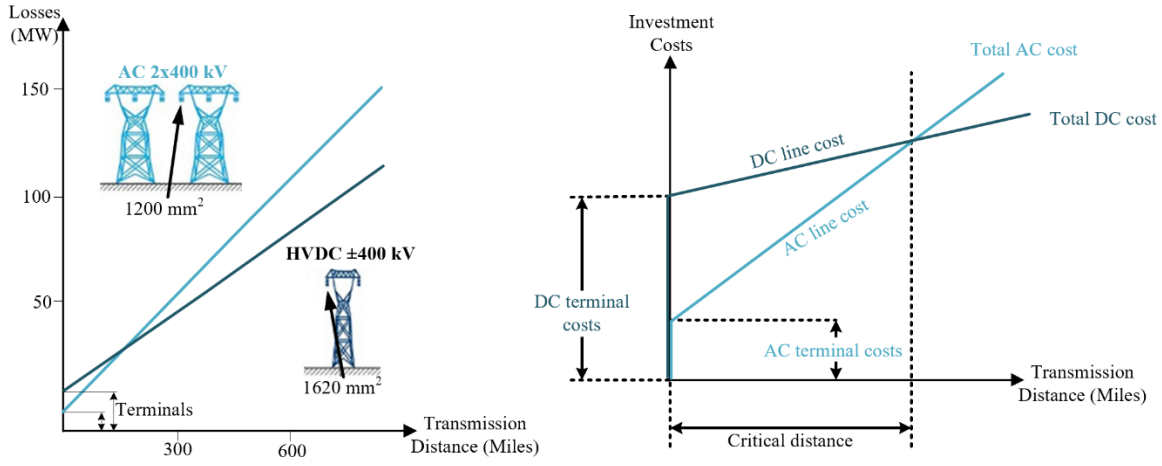

Figure 8. Comparison between overhead HVAC and HVDC lines; (a) losses; (b) cost [8]

AC transmission line equivalent circuit

In general, an AC transmission line (TL) can be characterized by its resistance, inductance, capacitance, and conductance, and the equivalent circuit of the TL can be created with the distributed parameters as shown in Figure 9 where *R* and *L* are resistance and inductance per length unit, respectively, *C* and *G* are capacitance and shunt conductance per length unit, and *V* and *I* are the voltage and current at the *x* distance of the line.

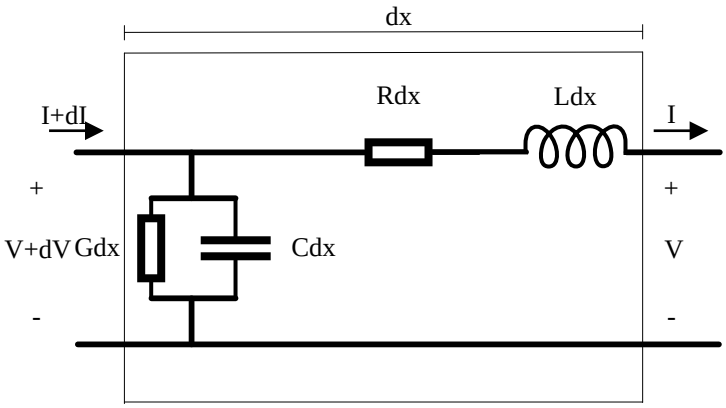

Figure 9. Transmission line equivalent circuit with distributed parameters

TL equivalent circuits with distributed parameters are usually used for the EMTP studies, where the propagation speed is of interest. For the purpose of the analysis considered in this thesis, a simplified model would be more appropriate. There are many different equivalent circuits, of which the most common is π circuit.

To get the π circuit the line is divided through its transversal parameters and distributed elements are grouped into three elements, a series impedance between two shunt admittances as depicted in Figure 10. Depending on the line length the equivalent circuit can be simplified even more. For the short transmission lines (<50 miles) admittances can be neglected thus the equivalent model of the line consists only of *Z*.

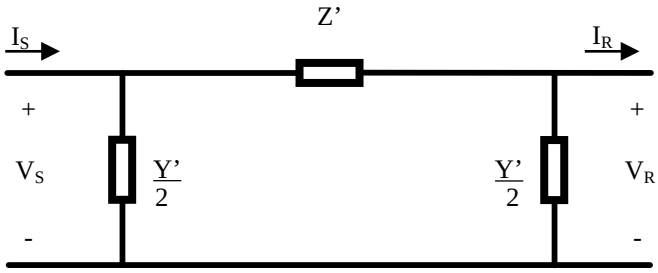

Figure 10. Transmission line π equivalent circuit

HVDC line equivalent circuit

A point-to-point HVDC system consists of three main components: two converter stations and DC line or cable. At one end of the line, AC is converted to DC via *rectifier* and at the other end, DC is converted back to AC via the *inverter*. Depending on the design of the converter station, there are three types of the HVDC converters: 1) Natural (Line) Commutated Converters (LCC), 2) Capacitor Commutated Converters (CCC) and 3) Self Commutated Converters using Voltage Source Converters (VSC). VSC HVDC has a list of advantages over the other two types and is a preferred choice nowadays for all but the highest power transfer applications. A VSC converter acts as a current regulated voltage source and can independently control both real and reactive power flow on the AC side line. Thus, DC line in the grid model developed in this thesis will be represented as a controlled voltage source.

2.2.4. Load

Load consist of a large number of individual devices that are always changing. Due to complexity and insufficient information regarding the load, for the purpose of the transmission system studies, loads are usually aggregated. Again, depending on the type of the studies and the answers that need to be obtained, different aggregated models exist. The two most common models are constant power (1) and constant impedance (2). The combination of those two with constant current loads is called ZIP.

$$S_i = P_i + jQ_i \tag{1}$$

$$S_i = \frac{|V|^2}{Z_i} \tag{2}$$

In this work, a constant power model will be used.

2.2.5. Shunts

Besides the main network elements listed above, the power grid also includes other devices such as shunt capacitors, reactors, and power electronic reactive control devices. These devices are used to control reactive injection into a given bus, and as such help maintain and control voltages at that bus. These are elements used by system operators to maintain defined operating voltages throughout the system. Capacitors and reactors are passive, meaning that their reactive output is going to be a function of the bus voltage, whereas power electronics can control to a set voltage, and as such, vary their reactive output independent of bus voltage.

2.2.6. Bus

A bus is a point of interconnection of electrical devices. There are three types of buses in the power system model within the context of a power flow: PQ bus, PV bus, and a Slack bus. Most of the buses in the power system are modeled as PQ buses. They are also called load buses. PV buses (generator buses) have known power output as well as voltage magnitude set point, and usually, those nodes have some sort of controllable reactive power resource in order to maintain the voltage magnitude. For the power system studies, only one bus is designated to be a slack bus and it has a fixed voltage magnitude and angle.

2.3. Power Flow Analysis

In this section, a quick overview of the power flow analysis is presented.

The power flow (sometimes called load flow) is the analysis of the flow of electric power, voltages, and currents in normal steady-state operation. Power flow studies are used for planning and expansion as well as for finding the best operating point of the current system. Based on the generator states and the system topology (transmission network structure), power flow finds the steady-state operation point ignoring the system transient processes. It calculates the voltage and phase angle of each bus and real and reactive power flow on each line as well as associated real and reactive power losses on lines and in equipment."

For the purpose of power flow analysis, transformers, transmission lines, and shunts are represented by their equivalent circuits consisting of *R*, *L*, and *C* and build the linear part of the network, whereas

generators and loads are treated as nonlinear components. The mathematical model of the power flow problem is formulated as a set of nonlinear equations independent of time (no differential equations).

In linear network relation between all the bus current injections and bus voltage is given by following node equation:

$$I_i = \sum_{j=1}^{n} Y_{ij} V_j \quad i = 1, 2, ..., n \tag{3}$$

or combining all modes in matrix form as:

$$\mathbf{I = YV} \tag{4}$$

where I_i and V_j are injected current at bus i and voltage at the bus j; Y_{ij} are the elements of the admittance matrix $\mathbf{Y}$ of $n \times n$ size where n is the number of the nodes in the system. In general, $\mathbf{Y}$ is a symmetric matrix except when the model includes phase-shifting transformers. Diagonal terms Y_{ii} are called self-admittances and are equal to the sum of all admittances of all devices incident to the bus i. The off-diagonal terms - Y_{ij} are equal to the negative of the sum of the admittances that are joining buses i and j respectively.

In the power systems, complex values of the voltage and current are not known, but rather complex power consumed by the load and the power injections at the generator buses along with the bus voltage magnitudes. The relation between injected current and power at the node is given as:

$$S_i = P_i + jQ_i = V_i I_i^* \tag{5}$$

where P_i and Q_i are the injected active and reactive power at node i respectively and where'*' represents the conjugate operator. Combining the equations (3) and (5) complex power flow equations are given as:

$$P_i + jQ_i = V_i \sum_{j \in i} Y_{ij}^* V_j^* \quad i = 1, 2, ..., n \tag{6}$$

Y, V and θ are defined as:

$$Y_{ij} = G_{ij} + jB_{ij} \tag{7}$$

$$V_i = |V_i| e^{j\theta_i} = |V_i| \angle \theta_i \tag{8}$$

$$\theta_{ij} = \theta_i - \theta_j \tag{9}$$

where G_{ij} and B_{ij} are conductance and susceptance between buses *i* and *j*, respectively; $|V_i|$ is the voltage magnitude, and θ_i is the voltage angle.

Using the equations (7)-(9), equitation (6) can be written as a set of two real power balance equations:

$$P_i = V_i \sum_{j \in i} |V_i| |V_j| \left(G_{ij} \cos\theta_{ij} + B_{ij} \sin\theta_{ij} \right) \tag{10}$$

$$Q_i = V_i \sum_{j \in i} |V_i| |V_j| \left(G_{ij} \sin\theta_{ij} - B_{ij} \cos\theta_{ij} \right) \tag{11}$$

For the *n*-bus system, there are *2n* real equation and *4n* variables (*P*, *Q*, |*V*|, and θ). Input data to a power flow problem consist of bus (node) data, transmission line data, and transformer data. For each bus, two variables are specified as input data and two variables are unknowns. Load buses have defined *P* and *Q*, whereas generator buses have *P* and |*V*|. As mentioned earlier, one bus (slack) has fixed |*V*|and θ. The slack bus does not exist in the actual power system but is required for solving the power flow (PF). The location of the slack bus influences the complexity of the calculations and usually is selected to be a bus with a large dispatchable generator.

Since it is non-linear, PF does not have an explicit solution, but rather it needs to use the iterative approach (numerical method) to obtain a solution that is within a predefined acceptable tolerance. A general approach used in the numerical methods consists of three main steps:

1) Initialize – initial “guess” of all voltages (magnitude and angle) at all buses (for PV buses, only the angle is initially guessed).
2) Obtain a new solution – using the power balance equations
3) Iterate until the pre-set condition is satisfied

Newton-Raphson

A very popular method for solving the PF is the Newton-Raphson method (NRM) that uses sequential linearization to solve the problem of the form: $\mathbf{f}(\hat{\mathbf{x}}) = 0$ where $\mathbf{x}$ is a vector of variables, voltage angles and magnitudes ($x = \begin{bmatrix} \theta_2 & \dots & \theta_n & |V_2| & \dots & |V_n| \end{bmatrix}$) and $\mathbf{f}(\mathbf{x})$ are power balance equations.

NR algorithm is given below:

$k = 0$
initialize $\mathbf{x}$
while $\left\|\mathbf{f}(\mathbf{x}^{(k)})\right\| > \varepsilon$ Do
  $\mathbf{x}^{(k+1)} = \mathbf{x}^{(k)} - \mathbf{J}(\mathbf{x}^{(k)})^{-1}\mathbf{f}(\mathbf{x}^{(k)})$
  $k = k + 1$
End while

Where:

$$\mathbf{J}(x) = \begin{pmatrix} \frac{\partial P_2}{\partial \theta_2} & \dots & \frac{\partial P_2}{\partial \theta_n} & \frac{\partial P_2}{\partial |V_2|} & \dots & \frac{\partial P_2}{\partial |V_n|} \\ \vdots & \ddots & \vdots & \vdots & \ddots & \vdots \\ \frac{\partial P_n}{\partial \theta_2} & \dots & \frac{\partial P_n}{\partial \theta_n} & \frac{\partial P_n}{\partial |V_2|} & \dots & \frac{\partial P_n}{\partial |V_n|} \\ \frac{\partial Q_2}{\partial \theta_2} & \dots & \frac{\partial Q_2}{\partial \theta_n} & \frac{\partial Q_2}{\partial |V_2|} & \dots & \frac{\partial Q_2}{\partial |V_n|} \\ \vdots & \ddots & \vdots & \vdots & \ddots & \vdots \\ \frac{\partial Q_n}{\partial \theta_2} & \dots & \frac{\partial Q_n}{\partial \theta_n} & \frac{\partial Q_n}{\partial |V_2|} & \dots & \frac{\partial Q_n}{\partial |V_n|} \end{pmatrix} \quad (12)$$

The most complex part in solving the PF using NRM is the inversion of the Jacobian matrix $\mathbf{J}(x)$ because it requires high computational resources and it is time-consuming.

Fast decoupled method (P-Q)

Depending on the type of studies (planning, security, etc.) that use power flow, sometimes certain approximations are made in order to speed up the calculations. To simplify the Jacobian matrix and calculations, it has been recognized that the real and reactive power balance equations can be

decoupled. Coupling between real power and angle as well as reactive power voltage angle is not strong so those elements in **J** can be set to 0 (half of the elements are removed).

$$\mathbf{J}(x)=\begin{pmatrix} \frac{\partial P_2}{\partial \theta_2} & \cdots & \frac{\partial P_2}{\partial \theta_n} & & & \\ \vdots & \ddots & \vdots & & 0 & \\ \frac{\partial P_n}{\partial \theta_2} & \cdots & \frac{\partial P_n}{\partial \theta_n} & & & \\ & & & \frac{\partial Q_2}{\partial |V_2|} & \cdots & \frac{\partial Q_2}{\partial |V_n|} \\ & 0 & & \vdots & \ddots & \vdots \\ & & & \frac{\partial Q_n}{\partial |V_2|} & \cdots & \frac{\partial Q_n}{\partial |V_n|} \end{pmatrix} \tag{13}$$

These approximations are justified by recognizing that usually $R<<X$ and that the angle difference between two buses is small thus $\sin\theta_{ij}\approx 0$. This approach is much simpler and more efficient, however, for the large system, that includes lower voltage model portions, the assumption made about the relation between *R* and *X* is not correct any longer, and the problem can become ill-conditioned.

DC approximation

Due to nonlinearity, in some cases, the analysis of large networks via the AC power-flow model is not feasible, and a linear (but less accurate) DC power-flow model is used instead. DC PF makes the most extreme approximations: a) *Q* is completely ignored; b) all voltages are always set to 1p.u.; and c) line conductance is ignored. This makes the PF completely linear problem; thus, it can be solved directly (there is no need to use numerical methods).

DC power flow solutions are often used in the industry for calculating optimal power flow (the objective cost function is for real power flows), and as the solution for production cost modeling, both due to the simplicity in calculating linear power transfer distribution factor (PTDF), or the participation that each line would have due to power transfer between two areas. However, as it does not consider reactive flows, there can be line overloads that would not be seen without a full AC solution. Furthermore, the DC approach does not allow for any further analysis to take place other than a simple power flow.

2.4. Transient Stability

Power system stability refers to the continuance of intact operation following any disturbance. It denotes the ability of a system, for a given initial condition, to regain a state of operating equilibrium after being subject to a disturbance [9]. Disturbances can be small in the form of load changes that occurs continually, or large, such as loss of generator, or large load. Transient stability studies simulate alterations following disturbances or large sudden load changes. Models involved in this type of study reflect the transient stability time frame (up to dozens of *s* with the time step ranging from ¼ to 1 cycle). Transient stability simulations involve more detailed models than power flow, taking into account additional generator and switching dynamic changes and it considers electromechanical analysis. First swing stability (the ability for the generator to maintain synchronism following a major event) is considered, along with the general interactions that the generators, their control systems, and the transmission topology have with each other. A high-level view of the generator model and the system state variables that are exchanged among different models is shown in Figure 11.

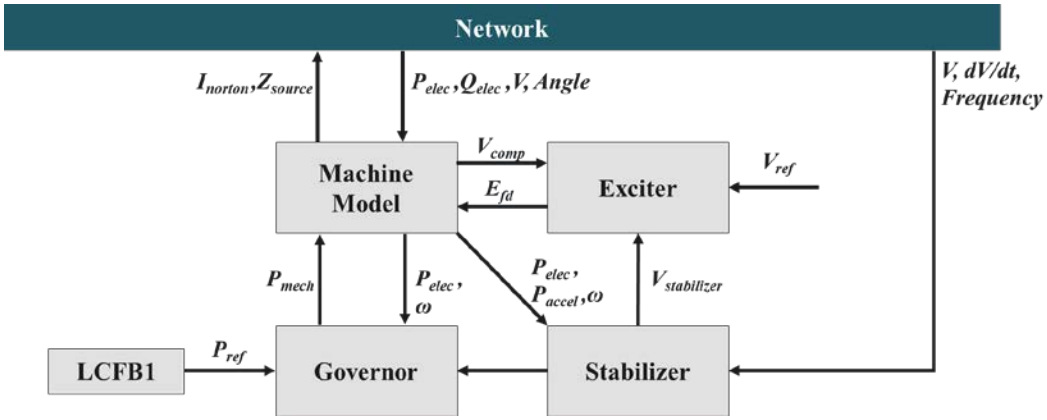

Figure 11. Generator dynamic model with the state variables [10]

Where the following nomenclature applies:

P_{elec} = electrical power
Q_{elec} = electrical reactive power
V = voltage at terminal bus
$\frac{dV}{dt}$ = derivative of voltage
V_{comp} = compensated voltage

P_{mech} = mechanical power
ω = rotor speed (or deviation from nominal speed)
P_{accel} = accelerating power
$V_{stabilizer}$ = output of stabilizer
V_{ref} = exciter set point
P_{ref} = governor set point

The time series delays that are associated with some of these control system (such as the delay time in the increase in mechanical power output following a governor action) is captured, along with enforcement of limits, ensuring that the generators stay within their designated capabilities.

Transient stability analysis will be conducted to study the dynamic behavior of the European grid before and after the Baltic States transmission system integration. Also, results acquired at this stage will serve as an input to the modal analysis tool for the further analysis and quantification of the behavioral changes.

2.5. Modal Analysis

Large interconnected grids have inter-area oscillations that occur when a group of electrically distant (having relatively high impedance) generators oscillate against each other at the low frequencies (0.1-1Hz). Interarea oscillations (also called natural oscillations) are related to a system topology and dynamic properties of the generators through the electromechanical modes of oscillations. Besides frequency, these modes are characterized by their damping and shape (magnitude and angle). When not properly damped, such oscillations could jeopardize the stability of the system and even cause a blackout [11]. In addition, the negative economic impacts which are a direct consequence of oscillatory behavior increase a need for tools that can detect and track them, in order to be able to design mitigation measures and reduce the negative influences.

The mathematical tool used to analyze the oscillatory behavior of the system is called modal analysis [12]. The goal is to estimate the mode's parameters (i.e., frequency, damping ratio, magnitude, and phase angle). There are two main approaches that can be used to study this phenomenon, 1) methods based on the system model and 2) measurement-based method. The first method is performed by calculating the linear matrix of the detailed system model and its components (including dynamic models). This is not always the best choice especially when analyzing a large network. The second, and preferred method (measurement-based) for this thesis uses the results (emulated measurements) obtained from the transient stability simulations to perform the calculations for modal analysis.

Furthermore, depending upon the system state when measurements are acquired there are two classes of the algorithms used for the estimation of the modes. When the system is in normal operating state (quasi-steady-state) oscillations are “hidden” in the system measurements and special techniques are used for the estimation (ambient based algorithms such as Least Squares, or Yule-Walker) [13]. On the other side, when there is a system disturbance (generator trip, or large load trip), modes can be estimated using so-called ring-down analysis.

Prony’s method was the first one used for modal analysis [14]. Since these phenomena became better understood, many other algorithms were developed, such as Hankel Total Least Squares, Dynamic Mode Decomposition, Matrix Pencil Method (MPM) to name a few. It has been shown that the MPM method has advantages over other methods, in terms of signal to noise ratio, and when dealing with signals with unknown parameters [15], thus it will be used in this thesis for the analysis.

The main idea behind the MPM is to estimate all mode parameters by fitting the measurement waveforms to a pre-specified signal model (a linear combination of the exponentially dumped functions) given in (14).

$$\hat{y}(k) = \sum_{i=1}^{M} R_i z_i^k + n(k);\ k = 0, \ldots, N-1 \tag{14}$$

Where:

$y(k)$	= observed signal
$n(k)$	= system noise
M	= number of desired modes
$R_i = A_i e^{i\theta_i}$	= complex amplitude
$z_i = e^{(\sigma_i + j\omega_i)\Delta t}$	= poles of the system
σ_i	= damping factor
ω_i	= angular frequency
N	= number of samples

Mode shape that is characterized by A_i and θ_i is calculated from the complex residues, whereas damping factor and frequency are estimated from the eigenvalues of the system poles z_i. Damping ratio and frequency can be calculated using the following:

$$\zeta_i = \frac{1}{\sqrt{1+\left(\frac{2\pi}{\sigma_i}\right)^2}} \frac{\omega_i}{2\pi} \times 100\% \tag{15}$$

$$f_i = \frac{\omega_i}{2\pi} \tag{16}$$

PowerWorld's Simulator has an add-on built-in tool with the MPM algorithms, and it will be used for all analyses.

Chapter 3: Recovery of AC Solution from the DC Solution

In this chapter, procedures for recovering an AC solution from the DC ENTSO-E case are studied. Two main problems are researched: what data needs to be in place to be able to get the realistic AC solution, as well as a heuristic approach on how to recover the solution. The chapter starts with a quick overview of the power system simulator used to build the model.

3.1. Power System Simulator

For the model development and other analysis conducted in this thesis, PowerWorld's Simulator (PWS) was used [16]. PWS is an interactive power system simulation and visualization platform designed to simulate and analyze transmission system operation on a time frame ranging from several minutes to several days. The Simulator was created in 1994 at the University of Illinois Urbana-Champaign by Professor Thomas Overbye and today is widely used in both research and industry environments. The simulator provides a wide range of advanced tools, such as power flow, optimal power flow, fault and contingency analysis, transient stability to name a few. It has a highly effective package capable of simulating systems of up to 250,000 nodes.

PWS provides a powerful visualization package that allows building contoured displays and it has an intuitive, interactive graphical user interface (GUI). Contouring allows and simplifies analyses of large amounts of information all at once. A contouring option window as shown in Figure 12 is used to control the contouring type, values (actual values of the variables, dynamic, calculated), scales, color schemes, etc., for all objects present in the oneline display. Contouring displays were extensively used to observe voltage and reactive power distribution and guide the author on how to recover an AC solution from DC as it will be presented in this chapter.

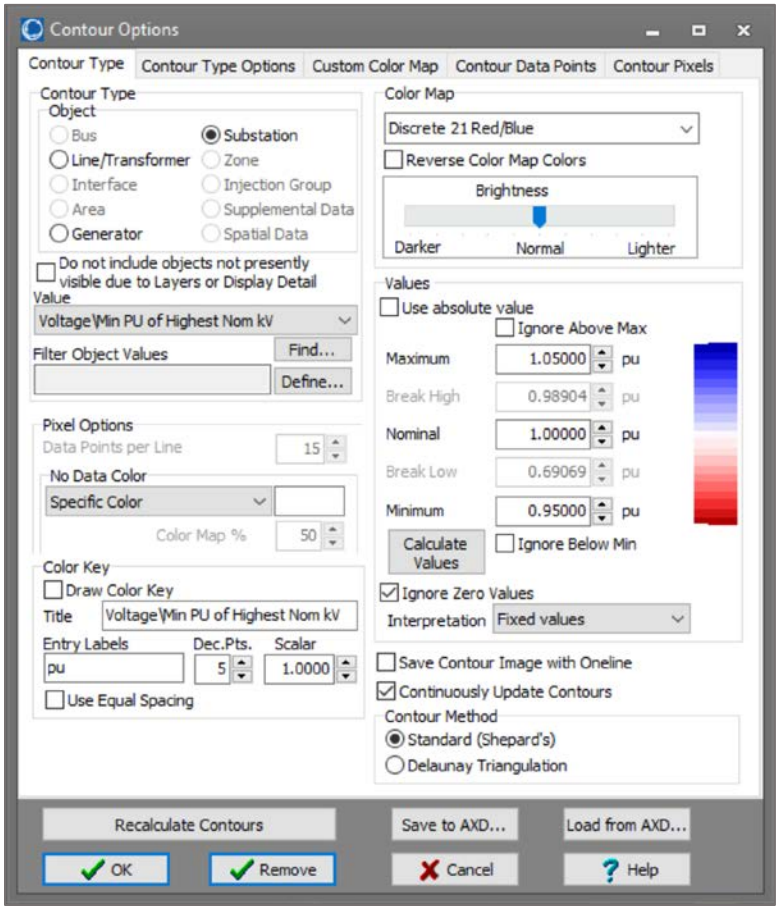

Figure 12. PWS contouring control window

Furthermore, the interactive GUI was extensively utilized for building the new transmission system of the Baltic Power System. PWS's oneline tools allow adding the network elements by directly using "Draw tools" (see Figure 13) and once the element is placed a control window automatically pops-up so one can input the model parameters and connections with other elements.

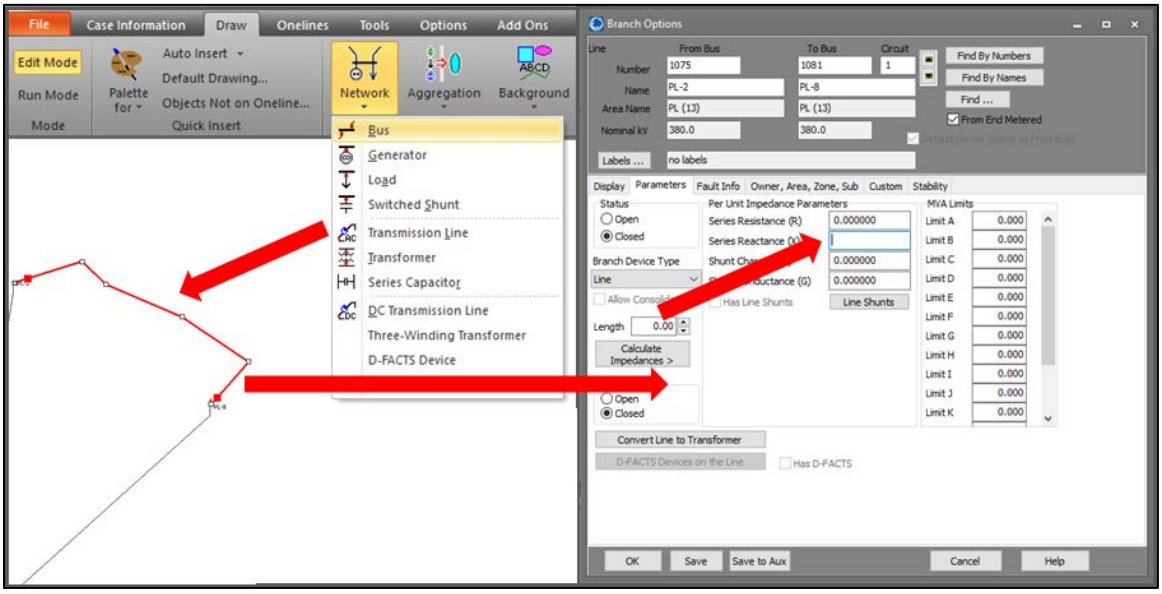

Figure 13. PWS draw and element control window

Additionally, Simulator provides access to the full Newton-Raphson method (iterative algorithms) with flexible capabilities in the solution process which was key in the recovery of an AC solution as discussed in this chapter including an optimal multiplier for the power flow solver. The optimal multiplier is a calculated step size which aims to prevent mismatch increasing between iterations [17].

3.2. Initial Case

For the purposes of this thesis, all of the models used came from publicly available data and material. The initial starting case was a DC model of the ENTSO-E power system that was developed in 2013, for the 2009 winter operating season [18]. This data was tuned to 95% accuracy in comparison with the actual published cross-flow values within Europe for 2009 [18]. The authors made this case publicly available on the PowerWorld website [19]. The oneline drawing is depicted in Figure 14.

The model consists of 1,494 nodes, 2,322 lines, 570 generator units with a maximum capacity of ~619 GW, and 1092 loads of total ~388 GW. The network is divided into 33 areas, and the total generation and loading of each area are given in Figure 15. A summary of the buses by the voltage level is given in Table 2. Table 3 gives a summary of all generator units in the initial case including total capacity, and the generation divided by the fuel type. Figure 16 shows the generation distribution based on the fuel type.

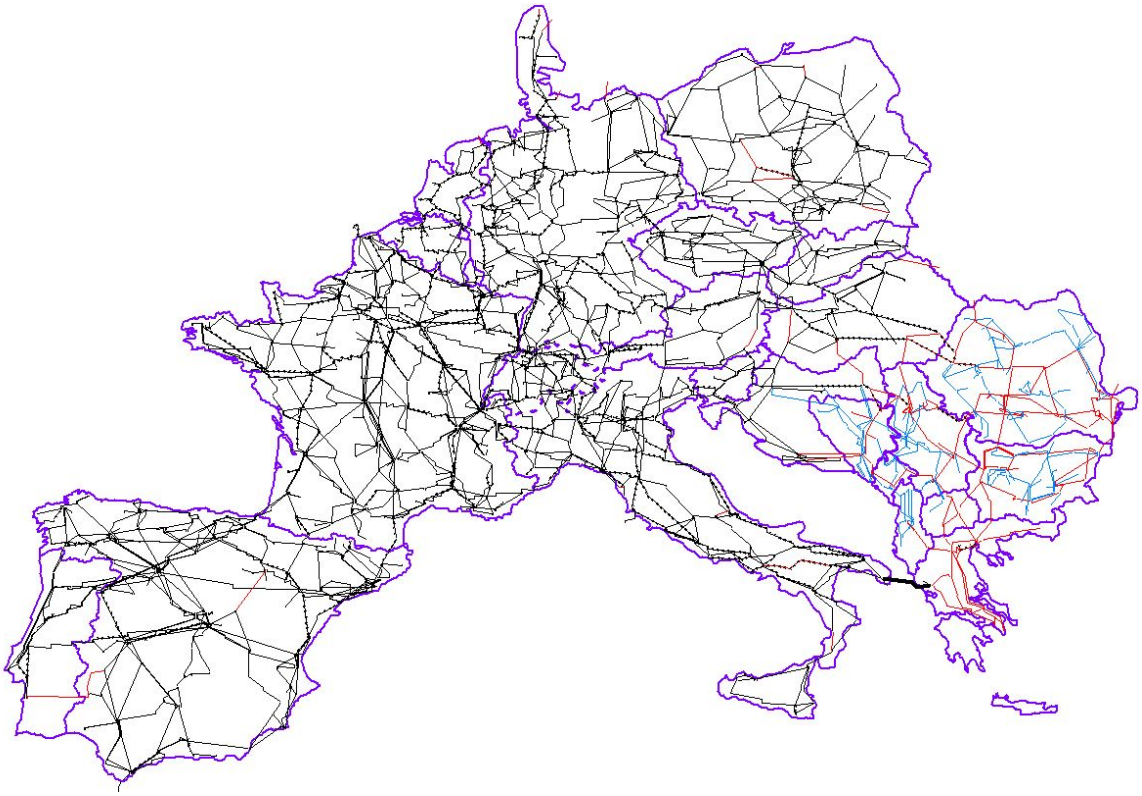

Figure 14. Oneline drawing of the ENTSO-E system [18]

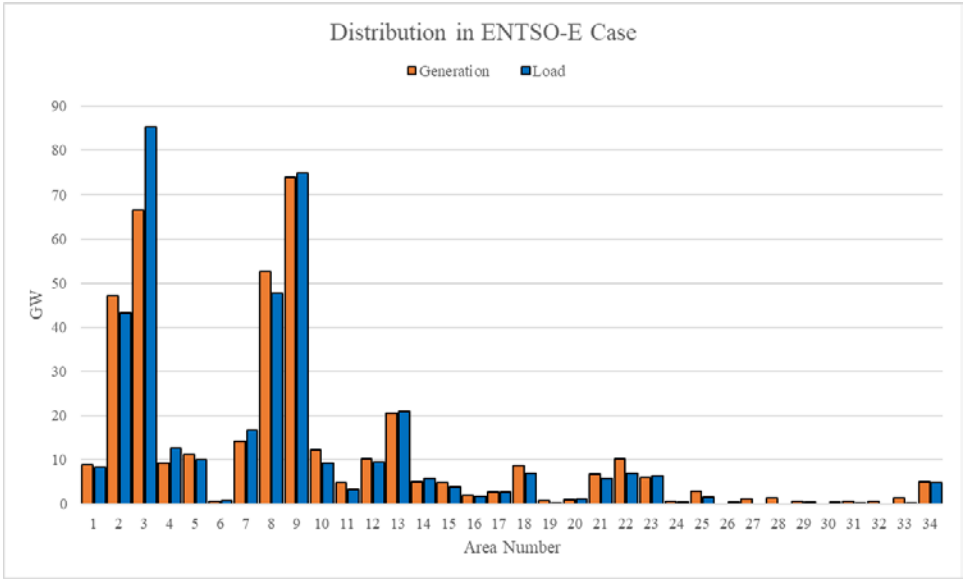

Figure 15. Total generation and load across the areas in ENTSO-E system

Table 2. Bus voltage levels in ENTSO-E system

Voltage Level	Number of buses
380 kV	1358
220 kV	133
138 kV	2
110 kV	1
Total	**1494**

Table 3. Generators type and capacity in ENTSO-E system

Fuel Type	Number of units	Total Capacity [MW]	Total Generation [MW]	Utilization [%]
Bituminous Coal	154	173,459.00	123793.70	71.37
Water	169	117,075.00	41,937.79	35.82
Nuclear	52	113,474.00	98,622.29	86.91
Natural Gas	95	113,273.00	80,966.06	71.48
Wind	43	52,158.00	15,517.28	29.75
Distillate Fuel Oil	37	30,868.00	21,699.24	70.30
Unknown	9	10,108.00	3,641.25	36.02
Solar	5	2,900.00	1,284.08	44.28
Wood	1	2,000.00	588.62	29.43
Water Pumped Storage	2	1,200.00	148.21	12.35
Geothermal	1	800.00	205.00	25.63
Waste Heat	2	600.00	122.70	20.45
Total	**570**	**617,915.00**	**388,627.60**	**62.89**

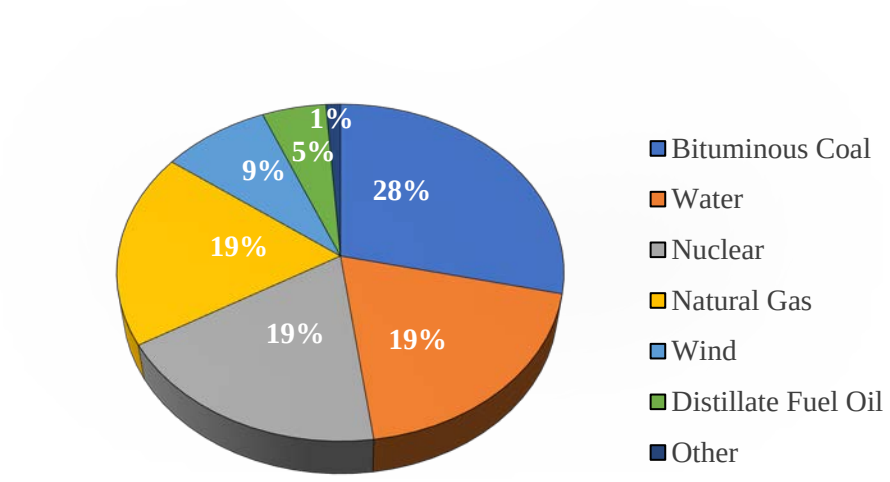

Figure 16. Generators distribution based on the fuel type in ENTSO-E system

As this was a DC model, the load values only had real MW values associated with them, the lines only contained reactive (*X*) values and no reactive capability curves were assigned to the generators. These were the key missing data which were necessary to build realistic π transmission line models as well as finding the AC solution.

3.3. Missing Data

3.3.1. Transmission Line Model Parameters

It will be pre-emptively stated that the data used to generate the missing data in the ENTSO-E model was based upon the US Grid, which operates at 60Hz, whereas the European grid is at 50 Hz nominal.

As mentioned, the original case had only *X* values assigned to transmission line models, and series resistance (*R*) and shunt charging (*B*) needed to be added in the model. Estimating the resistance value of the transmission line from the limited data available (conductor type, configuration, etc.) has been done before, most notably by Thomas Overbye while at the University of Illinois at Champaign, and recently at Texas A&M [20]. This has been done for the synthetic modeling work that was sponsored by ARPA-E [21]. In the referenced work authors recognized that the positive sequence resistance value (*R*) of a given line is tightly related to the positive-sequence reactance value (*X*) and the voltage level (*kV*) by analyzing the US Eastern Interconnection (EI) planning model. They calculated a median value, as well as the 10th and 90th percentile values for all lines in the EI model, and grouped them based on the voltage level, and the results are given in Table 4.

Table 4. Transmission line positive-sequence X/R ratio, for EI [19]

Voltage Level	**X/R Ratio**		
(kV)	**90%**	**Median**	**10%**
500	26.0	17.0	11.0
345	16.0	12.0	9.0
239	12.5	9.0	6.4
161	10.0	6.0	4.1
138	9.1	5.7	3.0
115	8.3	4.6	2.5

To analyze the results closer to the voltages that exist within the ENTSO-E (380kV) and the Baltic States (330kV) models, in this work, a WECC planning model was analyzed to determine the *R* values, by studying the *X/R* ratio from the 345kV transmission lines in WECC model.

In order to assign the values of *R* to each line, instead of using the distribution functions, a new fitting method is proposed. For 345kV voltage level, the line impedances from the WECC planning case were considered, and the relationship between *X/R* and initial *X* is plotted in Figure 17. From the plot, it can be realized that the best fit describing the relationship is an exponential function.

By closely examining the relationship between the *X* values and the line length in both the ENTSO-E and WECC cases it has been noted that the *X* values are ~20 times higher in the ENTSO-E case, which was an artifact of only needing the power transfer distribution factors (PTDFs) for the DC solution (with the only concern is the line parameters with respect to the others in the case to get the proper PTDF). As a result, all *X* values were scaled by factor 20. The decay starting at an intercept of 20 was chosen to set a maximum *X/R* ratio to be considered (a round number approximately one standard deviation from the 345kV class as shown in Table 4). This data will be applied to all current and future transmission lines (Baltic States) as the approximate voltage level makes up >90% of the total transmission lines in the cases.

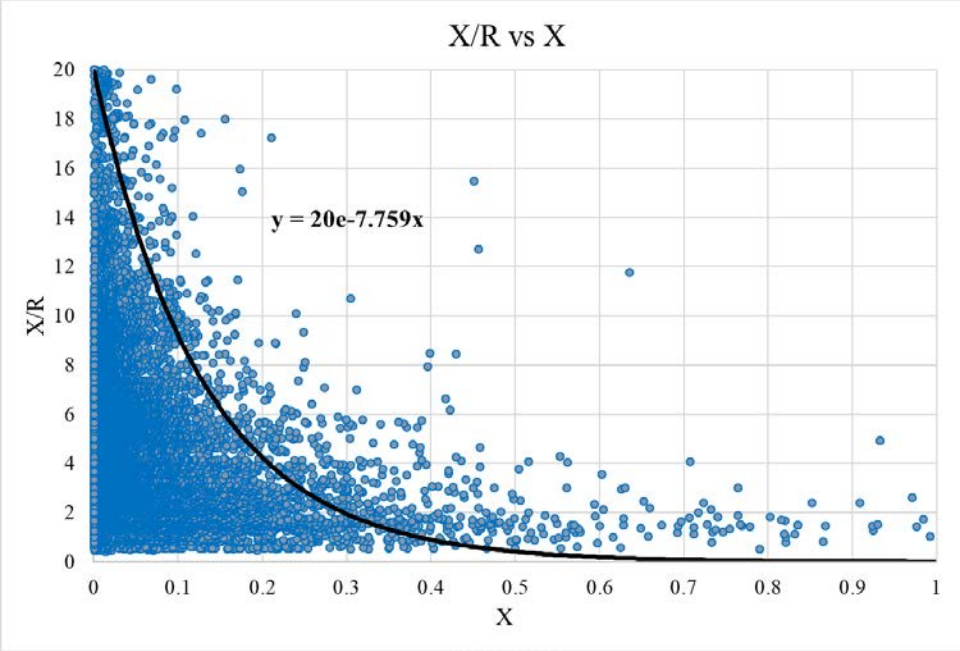

Figure 17. X/R vs X values for the WECC data

Using the estimated function, the ENTSO-E initial case was populated with the *R* values and the results are shown in Figure 18.

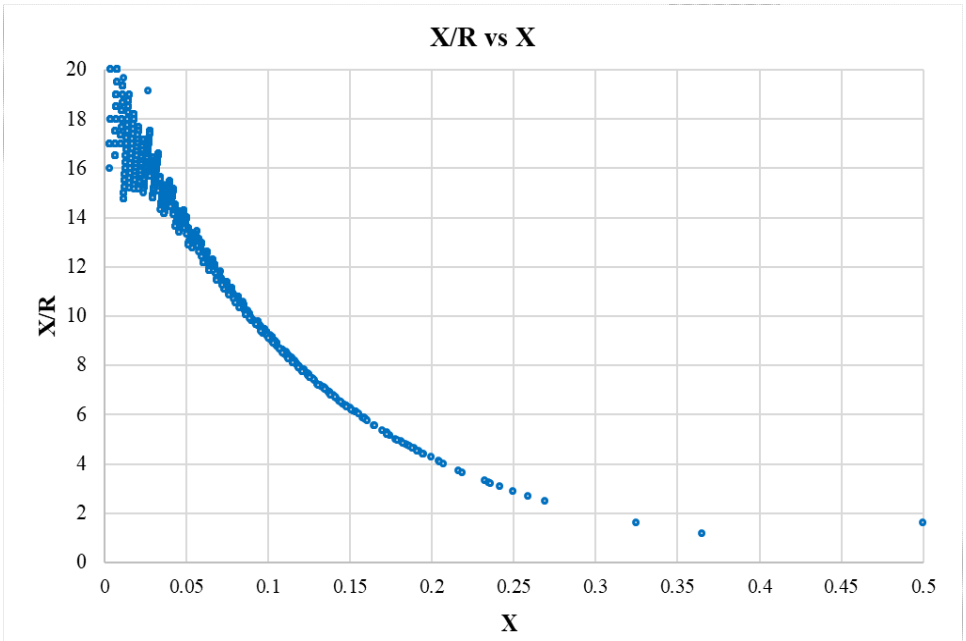

Figure 18. X/R vs X values applied to the ENTSO-E case

Using the same approach, shunt charging values are estimated by looking at the relationship between *B* and initial *X* (Figure 19) from the WECC data for transmission lines 230kV and higher (with the linear fit). The *B* values for 345kV lines are approximately 16 times that of *X*.

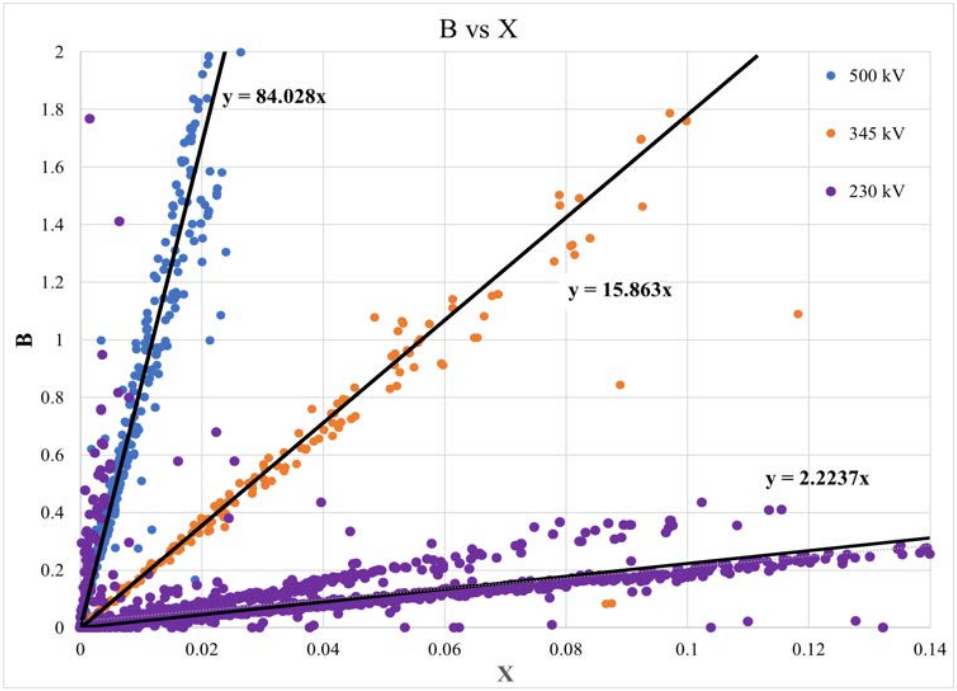

Figure 19 B vs X values (with linear fit) for the WECC data

Using the estimated function, the ENTSO-E initial case was populated with the *B* values and the results are shown in Figure 20.

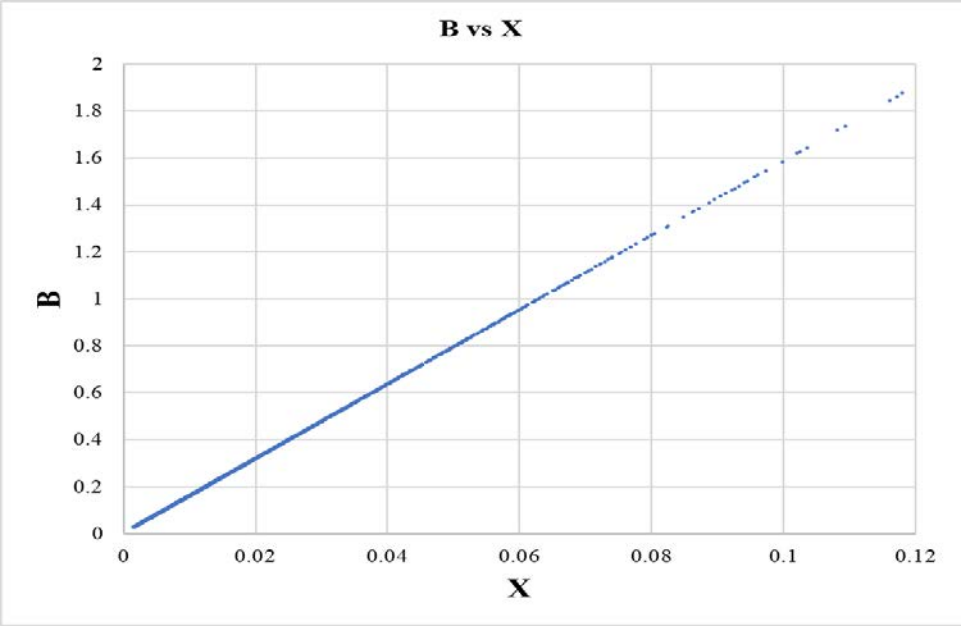

Figure 20. B vs X values applied to the ENTSO-E case

3.3.2. Reactive Load

To make a model more realistic, pure MW loads were converted to a load consisting of both, active and reactive portions. For simplicity, all loads were converted to a constant power with a fixed lagging power factor of 0.99 using equation (17), and the results are given in Table 5.

$$Q = P\tan(\arccos(Power\_Factor)) \tag{17}$$

Table 5. Load summary of the ENTSO-E case

Initial Case		**Updated Case**	
MW	MVar	MW	MVar
388,627.21	0	388,627.21	55,376.15

3.3.3. Generator Capability Curves

A necessary part of the AC power flow is the need to specify and set reactive output which a generator can provide. In order to maintain the voltage on the generator bus, the reactive power output of the generator varies. Regulating to a higher voltage requires more capacitive reactive power, however, generators do not have a limitless supply, but rather the reactive power outputs are dependent on the generator's capabilities curves and those should be included in the full AC solution.

Figure 21 shows the relation between the active and reactive power output of the synchronous machine with the excitation system. Very often, these curves are approximated by rectangular function as shown in Figure 21 with the red-dashed line.

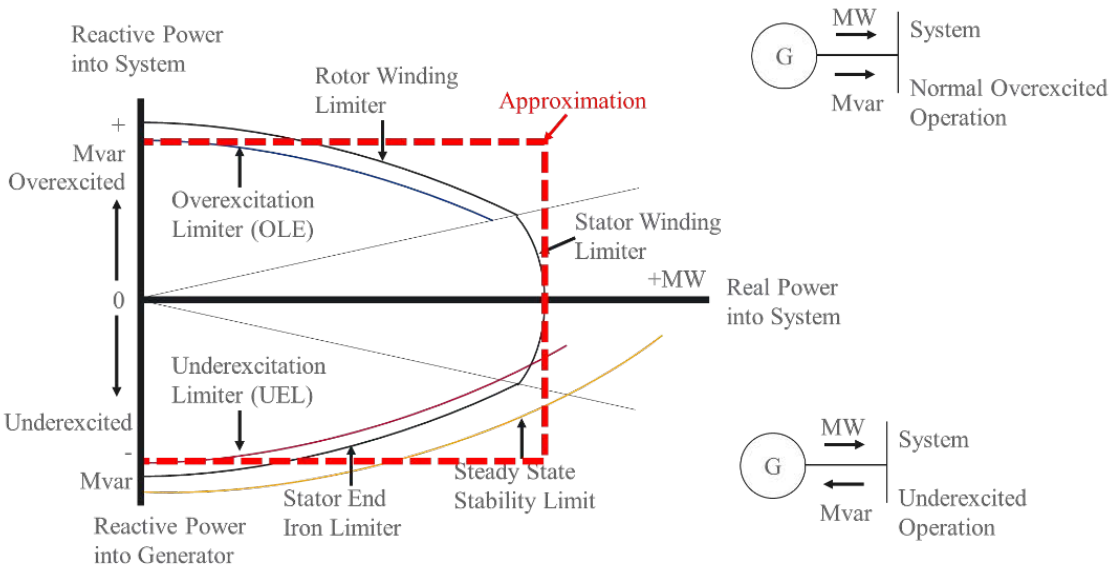

Figure 21. Generator capability curves and operating limits [21]

In this research, a simple approximation, by defining only min and max generator reactive power output for two extreme values of MW (0 and max generator MW output) will be used. To estimate the reactive capability limits for the ENTSO-E case the WECC data was, once again, used as a reference dataset. Figure 22 shows the distribution of min and max MVar limits in WECC as a fraction of the machine MVA base. Instead of a normal distribution, the average value for each limit (min and max) is calculated and results are given in Table 6.

Table 6. WECC Generator reactive capability ratios

Negative		**Positive**	
Mean	Median	Mean	Median
-0.333	-0.329	0.442	0.446

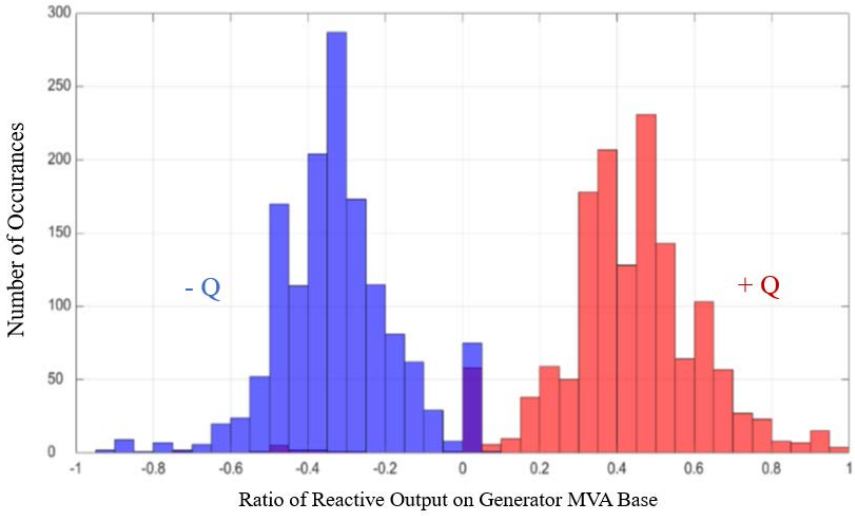

Figure 22. Distribution of MVar limits in WECC

These ratios are then used in PowerWorld Simulator as a simple multiplier based on the machine MVA base to populate the reactive capability curves which are defined via piecewise linear approximation as depicted in Figure 23.

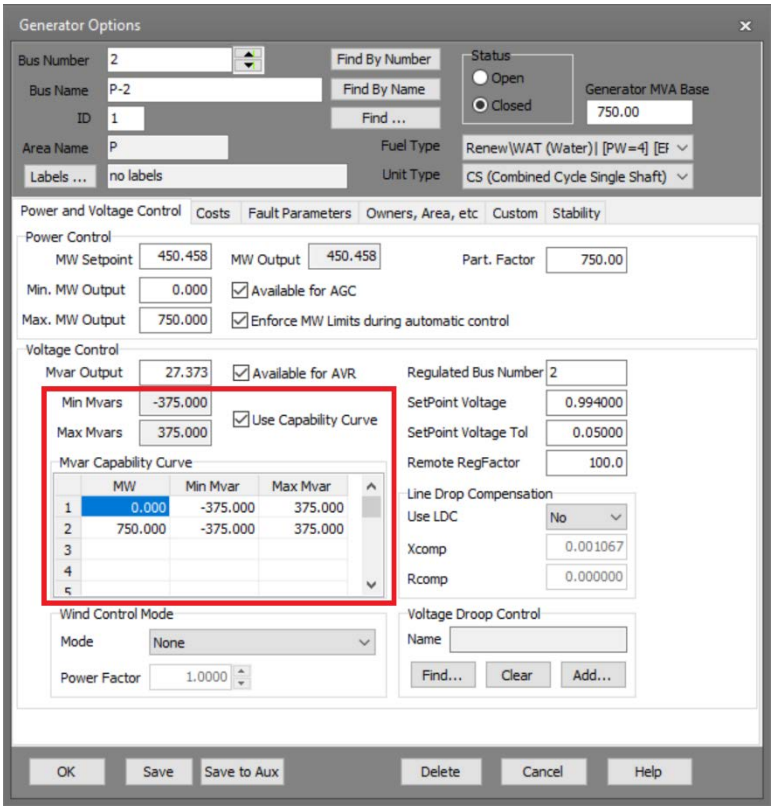

Figure 23. PWS generator control window

3.4. Iterative Solution

3.4.1. Overview

Recovering an AC solution from a DC solution is a difficult process that has been attempted by both industry and academia, especially in recovering an AC solution from production cost modeling, which solves the power flow as a DC [23], or during the initialization of large synthetic cases [24]. The major complications are the introduction of reactive flows, voltage regulation, and line losses. In order to be able to get a feasible AC solution, the updated model needs to have appropriate reactive support [24].That can be achieved by "hardening" the model by adding reactive sources (capacitors, reactors, tap-changing transformers, and generators) and by introducing proper coordination between those. Due to a reactive flow on the transmission line which adds to the current magnitude, power line losses (I^2R) are further exacerbated, thus the generator real power needs to be adjusted as well.

An often-considered approach is to simply reduce the overall load magnitudes to account for these line losses [25], but for the purposes of maintaining case integrity, the author believes that these losses should instead be covered by the online generation by ensuring that ample real power reserves exist to absorb the increased real power demand).

The solution proposed in this research is not mathematical, but rather procedural, following a series of prescribed steps to "ease" the system from a DC to an AC solution. The reason for this stepwise approach is that too big of a change in the Jacobian matrix from one solved point to another can easily result in a diverged power flow. As such, intermediate steps are taken (e.g. the addition of synchronous condensers, scaling of load and generation), as explained in the procedure below.

3.4.2. Procedure

Step 1: Observe voltage levels and MVar generation across the system

Once missing data (*R* and *B*) and reactive loads and reactive capability curves were being added to the model, it was possible to approximate the voltage drops that would occur from the generator sources (PV buses) to the load and intermediate (PQ) buses. To get the layout of what voltages would look like if all of the buses regulated by generation were set at 1.0 p.u., the reactive output of the online generation was set to "*unrestricted*" for the first initial AC solution (Figure 24). This first step allows one to identify the most critical regions that have the highest deviations from the nominal value.

Figure 25 shows a strong correlation between voltage values and reactive power of the generators after the first AC attempt.

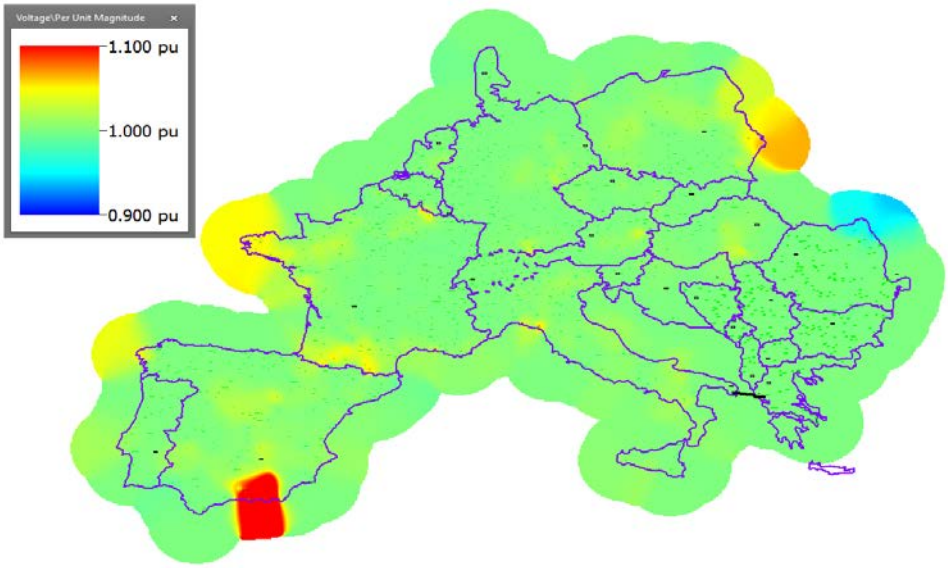

Figure 24. Voltage contouring from unrestricted generator reactive output

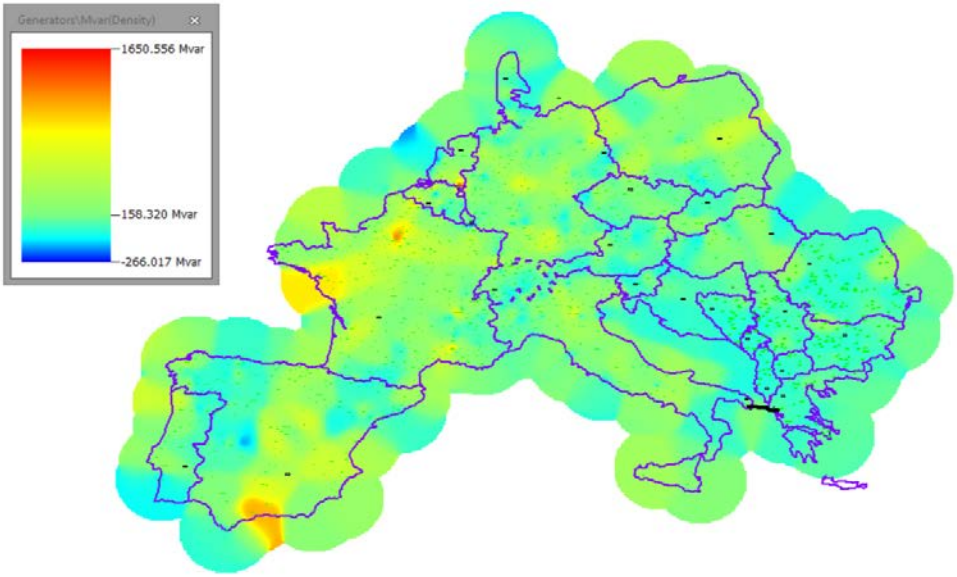

Figure 25. Generator reactive output when set to unrestricted

Step 2: Add synchronous condensers at every bus

After the initial network evaluation, the next step is to add synchronous condensers (SCs) at every bus as the first step in addressing the voltage regulation for an AC solution. The reactive capability of each condenser should be initially limited at +/- 9999 MVar, and the AVR setpoints set based on the current voltage of the regulating bus. The SCs are the only components that have automatic voltage

regulation enabled for reactive support. The generators AVRs are disabled but the automatic generator control (AGC) is enabled so that they can pick up real power due to losses.

In the topology, there are some buses which are connected to other buses via low impedance branches. Due to this, there is a need to introduce reactive current compensation (RCC) to prevent the possible reactive "fighting" between the SCs [23]. RCC is used to create artificial coupling impedance so that the machines will share reactive power appropriately and is mandatory for the stable operation (Figure 26).

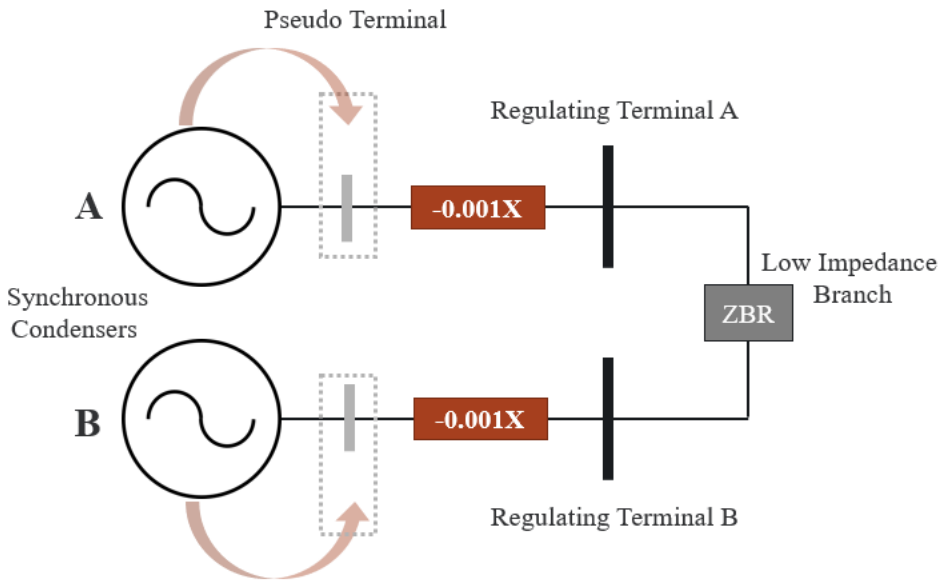

Figure 26. Reactive current compensation

By regulating a value that would be considered "inside" the machine, this added impedance allows each SC to regulate a different value than the bus in which they are connected. In this case, a value of -0.001 X (on generator MVA base) allows for equal sharing of reactive power and helps to prevent "circular flow" of MVars when some machines may be supplying and the other consuming. This is arbitrarily chosen as an initial value to provide for reactive sharing and is inconsequential as these SCs will be removed.

For an illustration, the AC power flow is solved with a high mismatch (>1000 MVA), and the associated reactive output from each SC is plotted via contouring corresponding to its reactive power output as depicted in Figure 27.

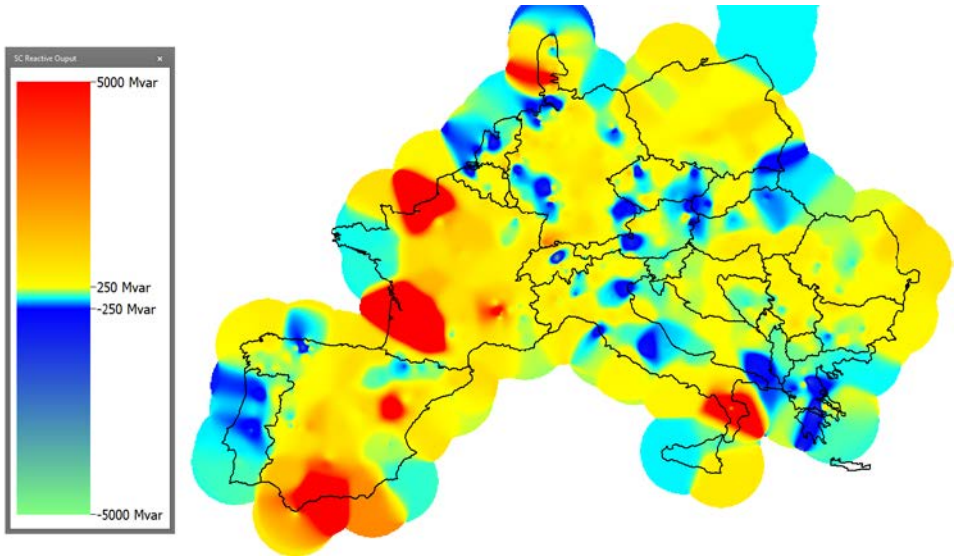

Figure 27. The initial output of the synchronous condensers when a high mismatch is allowed

Step 3: Reduce loads and generation

The next step is to decrease all of the loads in the system to a minimal amount. The idea is to maintain enough for each load to stay online at about approximately 1 MW. It should be noted that the original load values are saved separately to be used in recovery (Step 4). The generation output are also dialed back to values where it can respond to demand and cover for the losses based upon their maximum output (similar to steady-state governor droop). The initial value of the loads' density in the ENTSO-E case after the reduction is shown in Figure 28 (a high value of the load at the particular location represents the collection of multiple 1 MW load points).

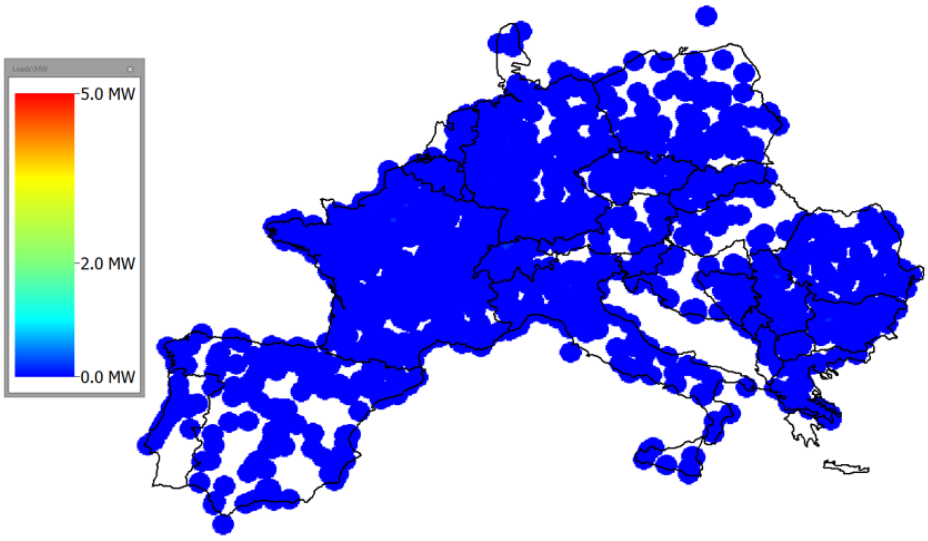

Figure 28. Minimal loading of the ENTSO-E case

Step 4: Reduce the solution mismatch

Next, through the iterative process, an AC solution is calculated while keeping all the load and generator values at a minimum and slowly reducing the mismatch allowed. In the first iteration, a large mismatch is enabled (1000 MVA) and then reduced in steps (10% of initial) until it reached 0.1 MVA. Figure 29 shows the generator loading with minimum load values for the ENTSO-E case and minimal mismatch.

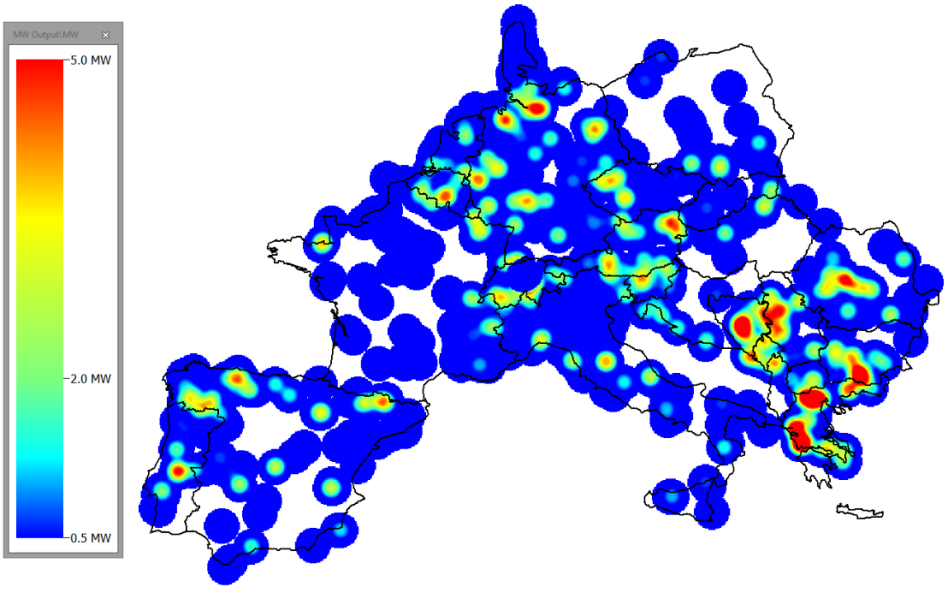

Figure 29. Generator loading with minimum load

Step5: Turn on generator's AVR and remove SCs

In the final step, all the SCs need to be removed and loads returned to initial values. To do so, at this point, all generator AVRs are enabled, with SCs AVR all being disabled. This still does not mean the SCs have stopped producing real and reactive power, rather it ensures that the generators and SCs do not cause instabilities due to control system oscillations as they "fight" each other to regulate to their setpoints. With the generator reactive capabilities set (Table 6), the generators AVRs are enabled, and the reactive output of the SCs are reduced, shifting the reactive power support to the generators. With the SCs taken offline and generation AVRs in place, the load is slowly brought back up to its original value in steps of 10% of the initial value.

Figure 30 shows the generation outputs of the final solved case and Table 7 summarizes the generation and load values of the initial and updated case and include the losses introduced by the added resistance and reactive flows.

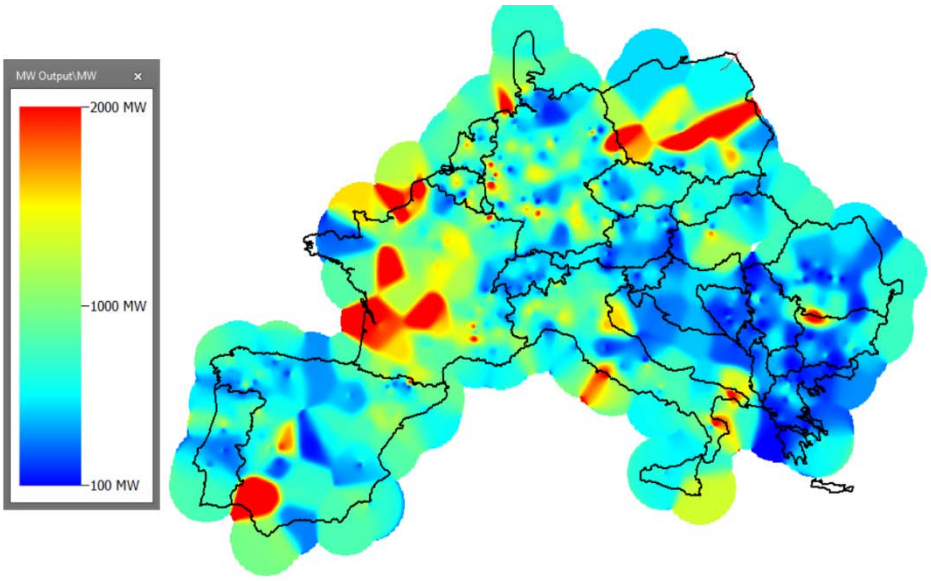

Figure 30. Generator output with recovered loads

Table 7. Load and generation summary of the ENTSO-E case with AC solution

	Initial Case (DC)	**Updated Case (AC)**
	MW	MW
Load	388,627	388,627
Generation	388,627	394,667
Losses	0	6,040

The given approach of the recovery of an AC solution from a DC solution is an extremely iterative process. It should be noted that this systematic solution is not implemented for maximum efficiency, but rather as a heuristic approach that is shown to work effectively for the purposes of this research.

Chapter 4: Building the Baltic States System

In this Chapter, a procedure for building a model of a grid from scratch is presented. The approach to building the Baltic State transmission systems consisted of four major parts: topology, transmission line parameters, system loading, and generation. Upon the completion, the model was connected to ENTSO-E system through one AC double circuit through Poland.

4.1. Topology

PowerWorld Simulator's oneline diagram builder was used to a great extent to build the basic system structure. First, an outline of the Baltic States (as a GIS"shapefile" - obtained from [26]) was loaded into PWS and it was modified to fit the geophysical properties of the already existing oneline diagram that was included as part of the original ENTSO-E case (Figure 14). It should be noted that this initial ENTSO-E case was not accurate with latitude/longitude, but only with respect to itself, thus Baltic States's shapefile needed to be scaled appropriately. Figure 31 shows the Baltic States and the portion of the ENTSO-E oneline.

Figure 31. Addition of the outline of the Baltic States to ENTSO-E

Next, the publicly available transmission map [27] was inserted in the oneline drawing as a background photo and aligned with the existing map as depicted in Figure 32.

Figure 32. Overlay of transmission map

After locating all the substations, using the drawing tool, the buses were added at each location. The total number of added buses (substations) is equal to 55. Next, following the transmission lines on the background map all the transmission infrastructure was built out. In total 71 lines were drawn. All substations voltages were set to 330kV and line impedance values were initially set to near zero (X = 0.00001 pu). These initial values are of no consequence, as they will all get repopulated. Figure 33 shows the transmission buildout of the Baltic States grid where green squares represent the substations.

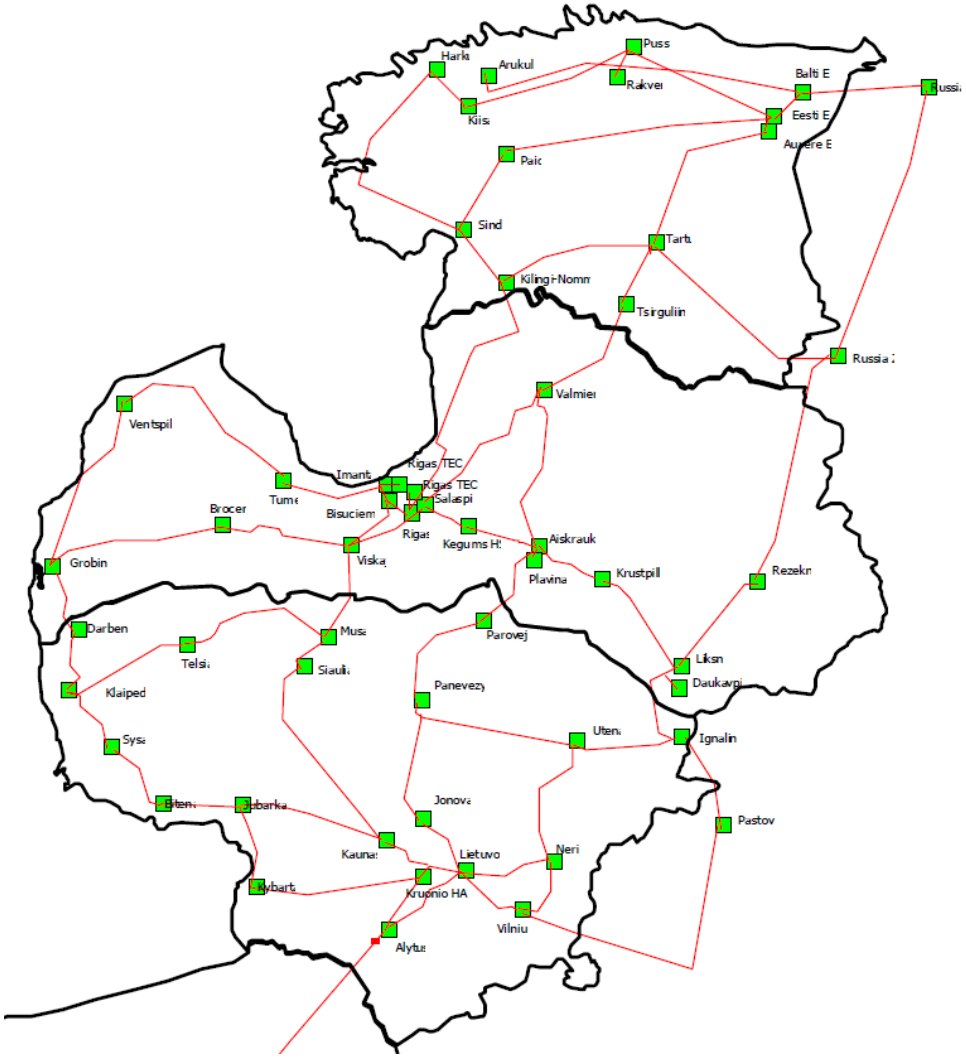

Figure 33. Transmission buildout of the Baltic States grid

4.2. Transmission Line Characteristics

In this section, transmission line model parameters are estimated, and the case is populated with the new values. Different from ENTSO-E initial case, all the transmission line parameters are now missing, including the series reactance values (*X*). With the assumption that the value *X* highly depends on the line length, first *X* values were estimated. The line topology and geographical location of the ENTSO-E case were used as a reference value. While the original oneline had no known concept of distance (other than the X,Y locations on the oneline), the “distances” could still be calculated and directly mapped to the Baltic States.

Figure 34 shows the relation between line length and *X* values of the ENTSO-E grid. While a few distinct correlations could be observed, the most concentrated correlation was used for determining line length versus a unit of distance for the Baltic States transmission lines.

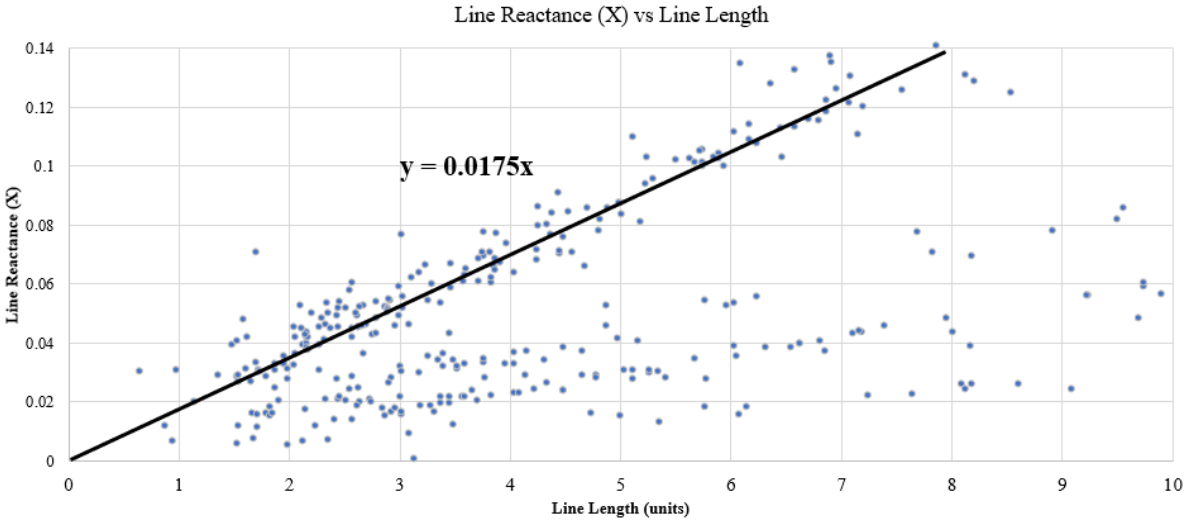

Figure 34 Reactance vs. Line Length

As PowerWorld measures transmission line distance based upon actual line distance and not the simple distance between substations (considers the actual route), closely following the transmission system geography in the building the Baltic system was shown to be beneficial. The data from the ENTSO-E case was determined to have a value of 0.0175 pu X/unit of distance and this relationship was utilized to generate the reactance values of the Baltic transmission system. Series resistance values were calculated using the previously estimated relation between *X/R* and *X* ($y = 20e^{-7.759x}$). Shunt charging (*B*) values were added by using a similar approach finding $B = 16X$.

4.3. System Loading

Next, loads were placed on each bus in the Baltic States. To estimate the load values (real and reactive power), the fact that the population is highly correlated to load in that area is utilized. A population map was placed on top of the Baltic States transmission as shown in Figure 35.

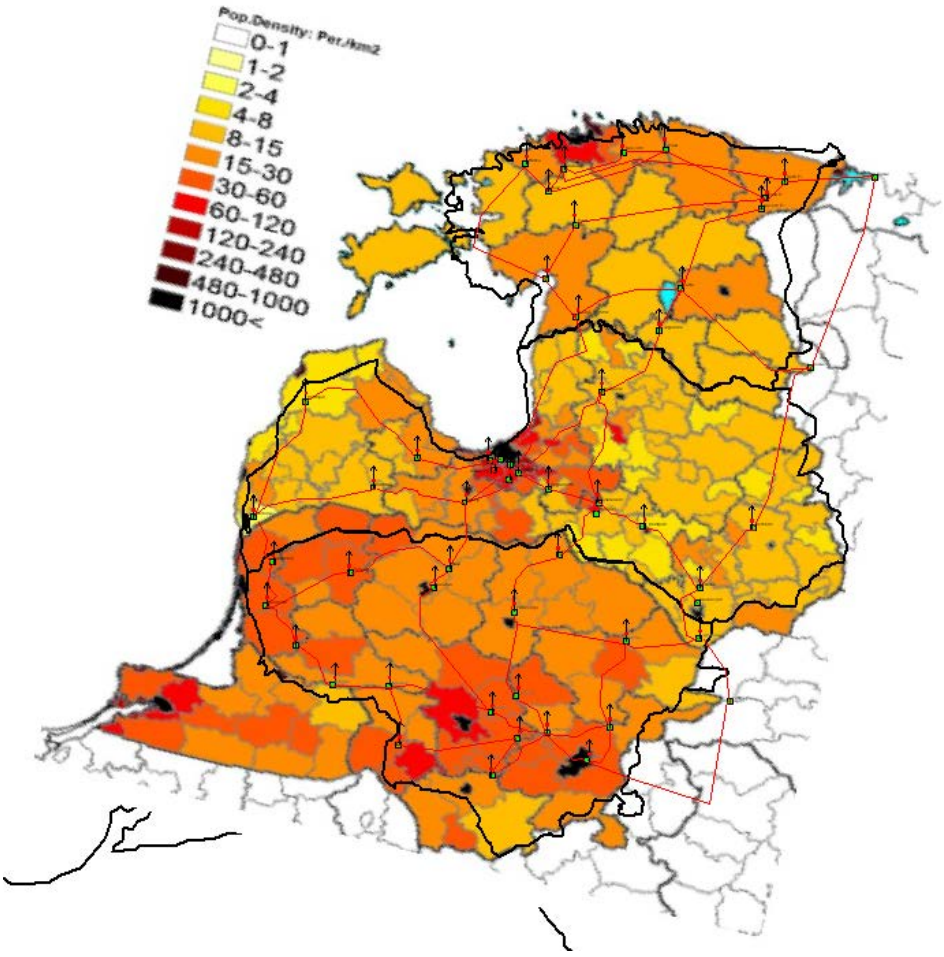

Figure 35. Overlay of the population density of the Baltic States on the oneline drawing [27]

A few assumptions were made to populate the load values. First, the total population is considered and divided into groups around the existing substations based upon population heating map. Next, it is grossly oversimplified that 2 people use twice the energy as one person, and then the relative weighting of the load of each region is estimated. Load weighting distribution is given in Figure 36. Figures 37-39 show the relative weighing for all load buses in each country. For this basic approach, industrial load will not be considered.

Next, using the system loading that is typically seen in all three country during winter peak [29-31], load values in region were normalized. Peak winter values are given in Table 8.

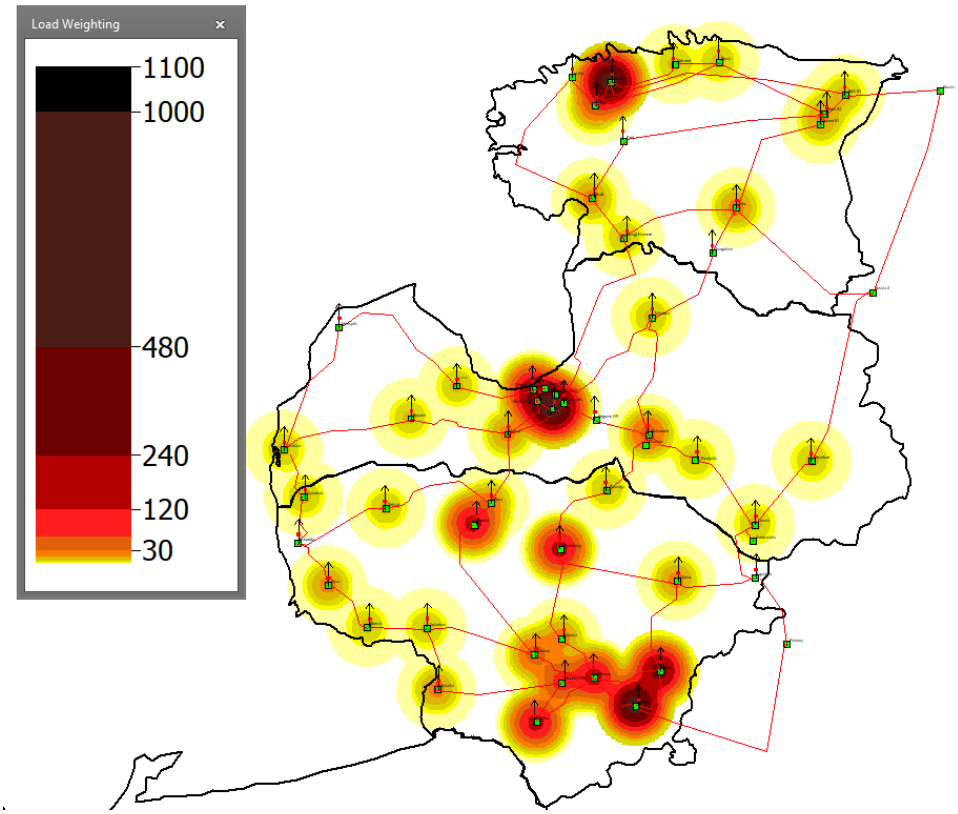

Figure 36. Load weighting distribution for Baltic States

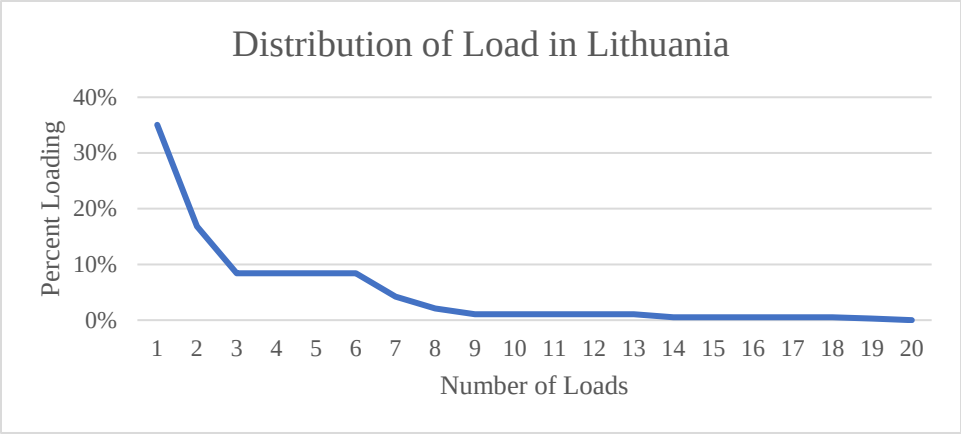

Figure 37. Relative distribution of load in Lithuania

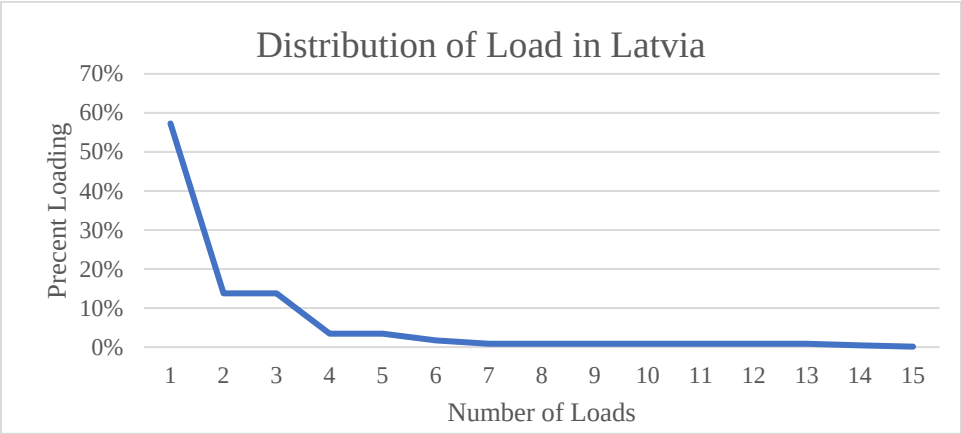

Figure 38. Relative distribution of load in Latvia

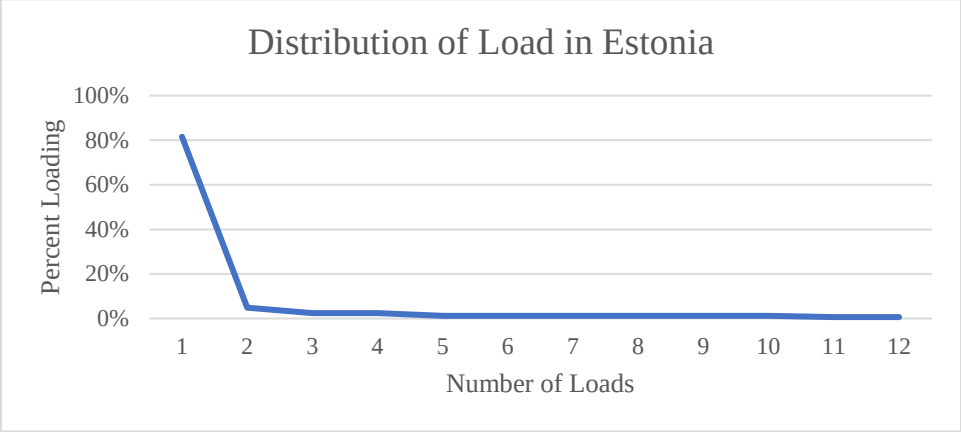

Figure 39. Relative distribution of load in Estonia

Table 8. Load winter peak values

Region	Peak Hourly Load
Lithuania	2,023 MW
Latvia	1,241 MW
Estonia	1,578 MW
Total	4,842 MW

Finally, using the relative distribution of load, total load is broken up as individual values at each bus as a percentage of the total load. Figure 40 shows the final loading of the Baltic States transmission system and it is summarized in the Table 9. The load was maintained at a given lagging power factor of 0.99, with the dynamic model being a simple constant *P*, constant *Q* (real and reactive respectively).

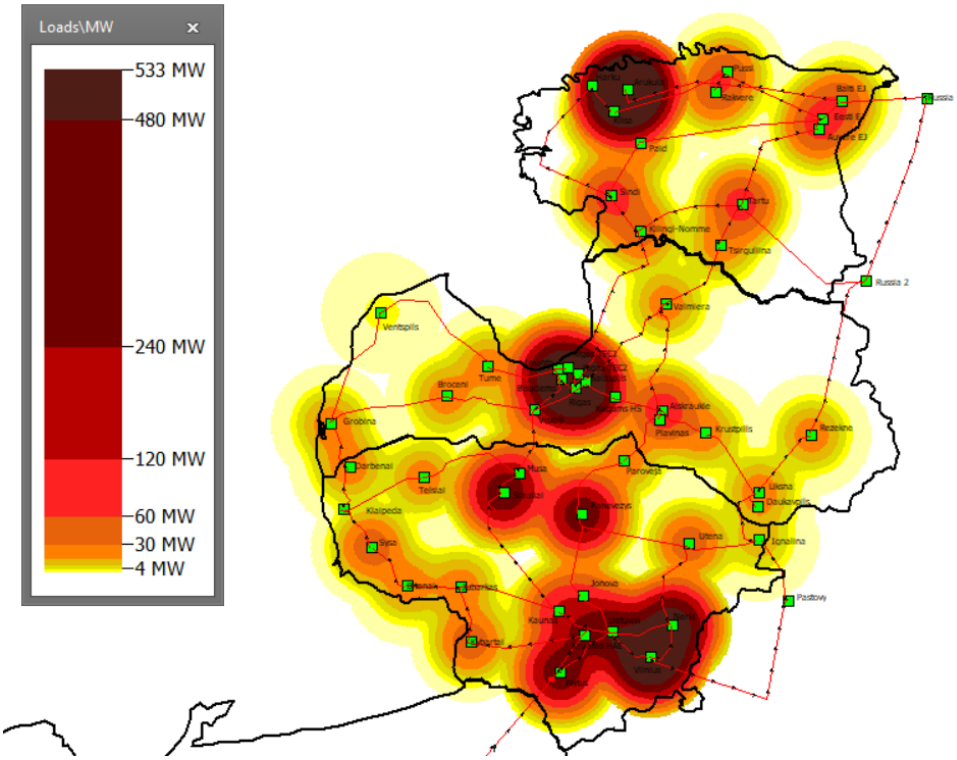

Figure 40. Loading in Baltic States

Table 9. Summary of the loads in the Baltic States transmission system

Region	Number of Loads	Load [MW]	[MVar Load]
Lithuania	20	2032	284.5
Latvia	15	1241	173.7
Estonia	13	1587	221.2
Total	**48**	**4860**	**679.4**

4.4. Generation

To include the generator information into the Baltic States transmission model, different publicly available sources were explored, [32-34], and the summary of generator units for each country are given in Tables 10-12. Geographical information for each generator was utilized as well, and in case of Lithuania, 7 generator units were placed at 6 buses, in Latvia in total 5 units were added, and for Estonia, total generation reported in Table 12 was divided between three buses. In addition, a fuel type was also recorded, thus the appropriate dynamic models for the machine and governor could be chosen as it will be discussed in the next chapter.

Table 10. Generation data for Lithuania

Lithuanian Power Plants		
Power Plant	**Fuel Type**	**Capacity (MW)**
Lithuanian Power Plant	Natural Gas	1,955
Vilnius Power Plant	Natural Gas	360
Kaunas Power Plant	Natural Gas	170
Kruonis Hydro Power plant	Hydro	402
Kegums Hydroelectric Power Station	Hydro	264
Total		**3,151**

Table 11. Generation data for Latvia

Latvian Power Plants		
Power Plant	**Fuel Type**	**Capacity (MW)**
Riga Thermal Power Station 2	Natural Gas	832
Riga Thermal Power Station 1	Natural Gas	1,390
Plavinas Hydroelectric Power Station	Hydro	884
Riga Hydroelectric Power Plant	Hydro	402
Kegums Hydroelectric Power Station	Hydro	264
Total		**3,772**

Table 12. Generation data for Estonia

Estonian Power Plants		
Power Plant	**Fuel Type**	**Capacity (MW)**
Eesti	Oil shale	1,610
Balti	Oil shale	1,390
Iru	Gas	190
Kohtla-Jarve	Oil shale	39
Ahtme	Oil shale	20
Diesel	Oil	9
Total		**3,258**

Figure 41 show the maximum generation available in the Baltics States region and Figure 42 show the total distribution based on fuel types.

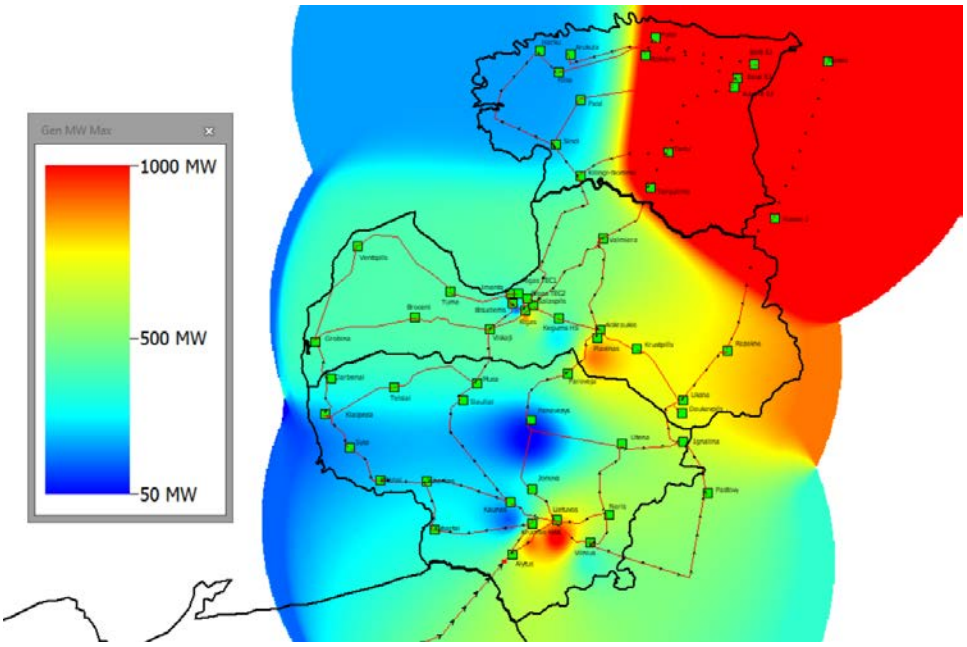

Figure 41. Baltic States generator maximum output

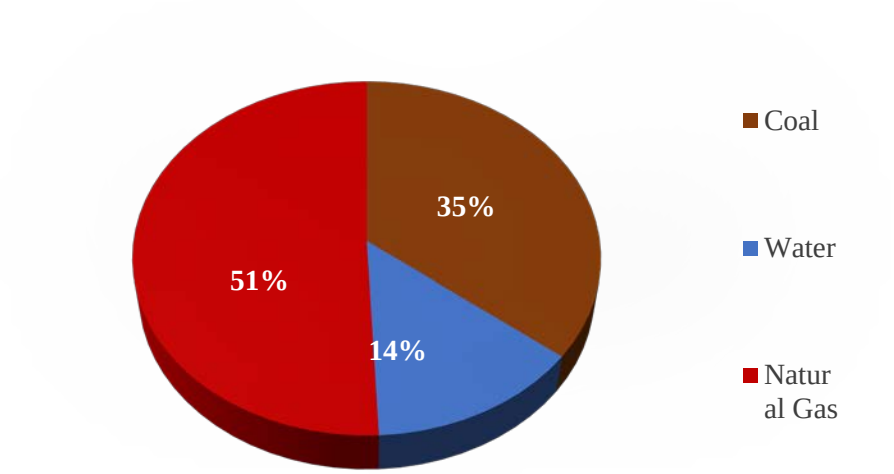

Figure 42. Generators distribution based on the fuel type in Baltic States system

4.5. Systems Interconnection

With build and solved case for ENTSO-E and Baltic States model, now both grids can be connected to get the proposed 2025 system topology to form the necessary foundation for analyzing system transient stability. The planned topology is as shown in Figure 43 and its implementation is given in Figure 44.

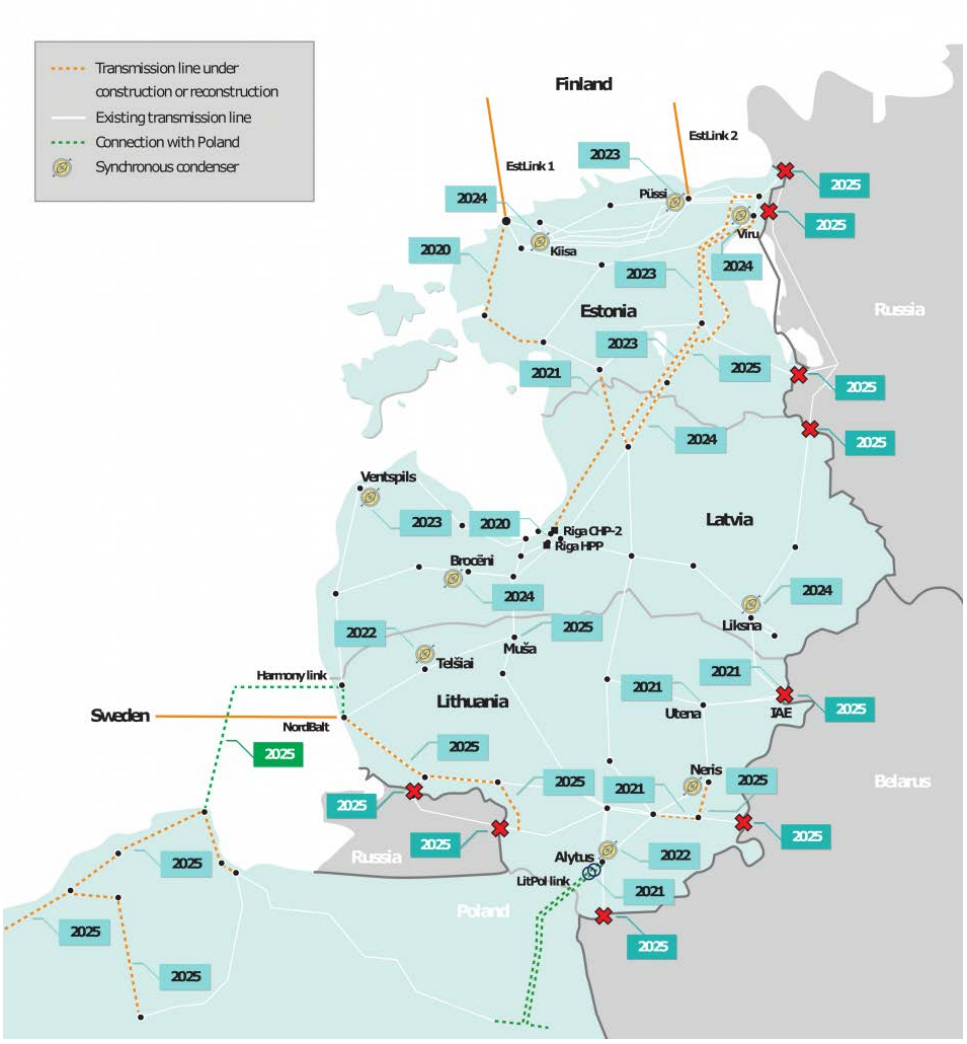

Figure 43. Planned Baltic State topology for 2025 [34]

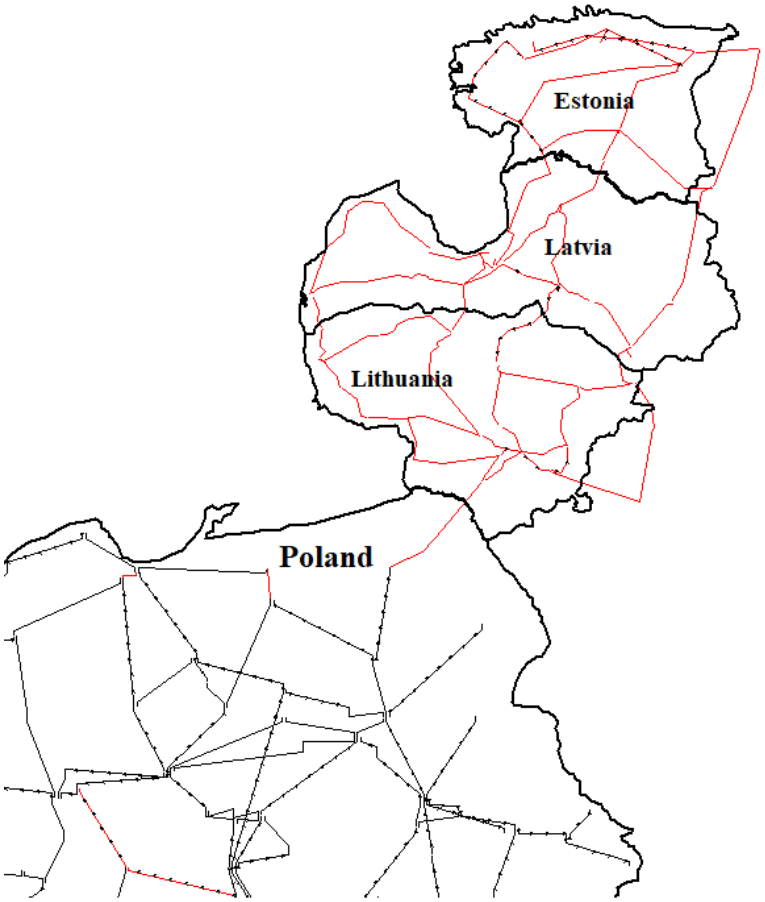

Figure 44. Implementation of 2025 topology

Due to the nature of access to the actual system data (and associated NDAs), and complexity of using open-source (but low visibility) data, no validation of this reduced-order system was performed.

Chapter 5: Dynamic Analysis

Until now, the built models are adequate for the steady-state like analysis such as power flow. However, to perform the dynamic analysis, the power system model needs to be expanded to include the machine dynamic information. The necessary dynamic data for the generation facilities does not exist for the ENTSO-E and Baltic system models used here, as such new models must be populated for the machines, exciters, governors and the power system stabilizers.

5.1. Missing Data

5.1.1. Machine and Governor Models

The data given for the generator types in Figures 16 and 42 were used as the basis for both the machine and governor models. For the purpose of this thesis, generator units were divided into three major types: turbine, hydropower, renewable. For each group, a standard dynamic model was assigned to units.

Turbines

The turbine-type models were assigned to all thermal power plants (coal, nuclear, fuel oil) which use steam, and all combustion generators. For high-speed turbines which rotate at about 3600 RPM (for 60Hz) the round-wound rotors are used (Figure 45), and the classical machine model for these turbine generators is the GENROU (round rotor generators). For the governor model, the TGOV1 (turbine governor) is chosen as it includes both steam and gas as the input to the generators. (as gases, superheated steam and natural gas have a comparable fluid viscosity).

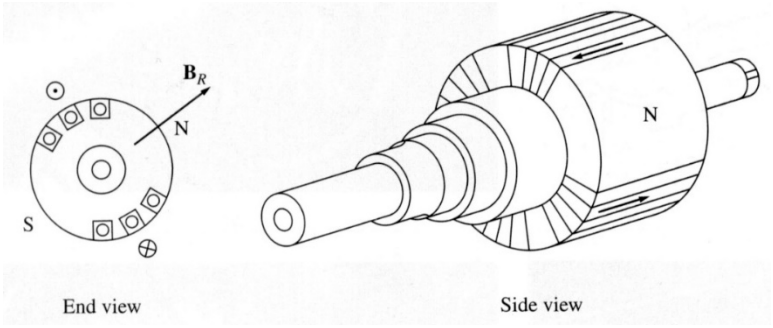

Figure 45. Two pole round rotor [36]

Hydropower

Hydropower plant turbines (water) are more efficient at much slower speeds are typically rotating at 200-300 RPM. The general machine model - GENSAL (salient pole – Figure 46) is typically used in

power system studies to represent these types of generators. The classical dynamic hydro power governor model is HYGOV model and it was assigned to all hydro generators in the combined ENTSO-E and Baltic States system.

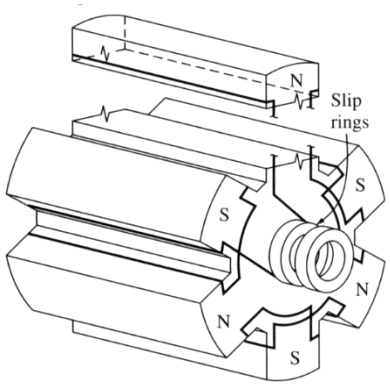

Figure 46. Six pole salient rotor [36]

Renewables

Wind/solar generation are all represented as full inverter-based resources using the WT4G dynamic model (type 4 wind turbine with full converter model). No governors were assigned to wind/solar plants.

5.1.2. Excitation Systems and Stabilizers

Exciter and power system stabilizer models for synchronous generation are the ESST1A (IEEE type ST1A excitation system model) and PSS2A (IEEE dual-input stabilizer model). These were chosen based on the large saturation of these model types in the WECC dynamic data, with the same models chosen for all synchronous generation for simplicity.

The associated WT4E exciter (electrical control for full converter wind-turbine generators) is chosen for the renewable generation units and no PSSs were added. Parameters for all the models are then populated using typical “default” values that PowerWorld Simulator provides.

5.2. Case Studies

The natural frequency of the European power grid has been well documented and is becoming more understood by the system operators due to the impact that it has on system stability. For the purposes of the thesis, small signal stability is not being performed, rather, transient ringdown analysis were conducted to determine changes that occur with these oscillatory modes for different topologies.

To demonstrate the value of the developed model, transient stability analyses are performed on the interconnected model to analyze both the impact of the Baltic States on the dynamic stability of the interconnected grid and the impact of events in the European grid on the Baltic States through the synchronous connection via a radial line.

In initial comparison, the Baltic State portion of the grid will be left disconnected (making it only the ENTSO-E model). The reason for this is twofold: 1) provide a method of direct comparison to the current known data and 2) provide a baseline to which the impact of the Baltic State grid for which it could be compared.

There are two major scenarios that will be analyzed, both of which involve a large generator loss. One of these will be only for the isolated systems of ENTSO-E (for a baseline), while the other with the Baltic States connected. This will be from two points of view, looking at the impact that the Baltic States have on ENTSO-E, and likewise ENTSO-E has on the Baltic States.

It should be noted that while high voltage DC lines exist in the Baltic system, the inclusion of these (for both power-flow and dynamics studies) was ignored. This was due to the lack of modeling of the connecting countries (Norway, Sweden, Finland) that do not belong to CE interconnection, and the fact that the large amount of online generation in the Baltic States cover the required load. The simplification is also justified by the fact that the simplified models often used for modeling HVDC (LCC and VSC) are not very responsive to frequency deviation events [37] and thus would have minimal impact on the results.

5.3. Results

5.3.1. Case 1 - Baseline Study

To be able to perform direct comparison and quantify the impact of the interconnection of two systems, first, an event that would cause a ringdown of both the ENTSO-E system alone and then with the Baltic States connected needs to be defined. This event will serve as the baseline event to create a ringdown. For all the analyses presented below, a loss of a large power plant (3,000 MW) in western Germany was chosen as the baseline event since the loss can be visible across the entire grid.

PowerWorld Simulator's "Transient Stability" program is used to conduct all the studies. Simulation time step is set to ¼ cycle, with a 2nd order Runge-Kutta method of integration. In order to ensure a good case initialization, all events will take place at *t=1 sec* after the start of simulation. Frequency

contours of the baseline generation loss is shown in Figure 47 at *t=1+0.015 sec* (15 ms after the event), with the lowest value being blue, showing the location of the generator loss.

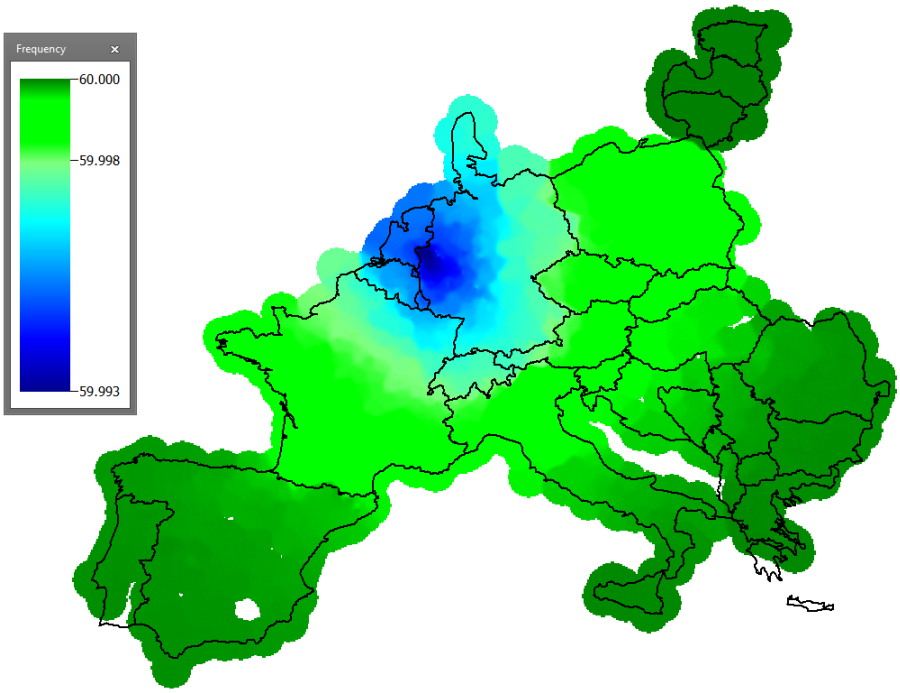

Figure 47. Frequency contouring of the generation loss event

This baseline case will be used to evaluate the effect of the event on the of the ENTSO-E system and also to determine the impact of an event occurring in ENTSO-E and the interconnected Baltic States. The time series plot of the frequency impacts of the event at the generator buses in the base case, are shown in Figure 48.

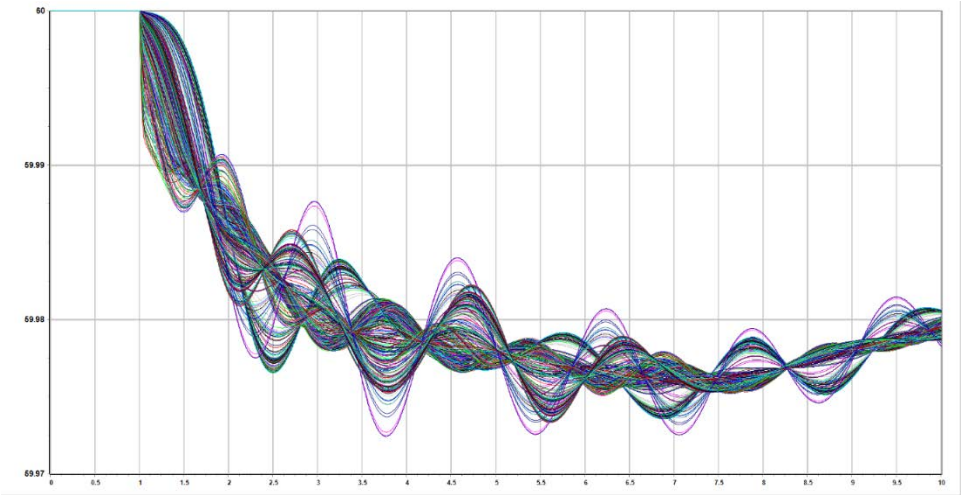

Figure 48. Bus frequency at all buses in ENTSO-E case for loss of generation event

To calculate the initial modes using the iterative matrix pencil method (MPM), time series data as shown in Figure 46 are loaded to a PWS's "Modal Analysis" tool. In total four modes were identified as well as the major participating signals (the ones where the modes have a highest amplitude), and the analysis is rerun with those signals being exclusively modeled (results shown in Table 13).

Table 13. Identified modes in initial ENTSO-E Case

Frequency (Hz)	Damping (%)
0.23	48.0
0.37	7.1
0.60	6.9
0.89	8.7

5.3.2. Case 2 – Interconnected Grid – Impact of the Synchronization

With the Baltic States interconnected with ENTSO-E, the effect of the same generation loss event on the synchronized system can be examined. In this section the impact of the Baltic interconnection on the response of the ENTSO-E will be examined by quantifying any changes in the modal behavior in the ENTSO-E portion of the grid (mode parameter changes or introduction of new modes).

Figure 49 shows the frequency response of the generators, now also including all generator buses in the Baltic States model (black time series representing the bus frequency in Baltics system).

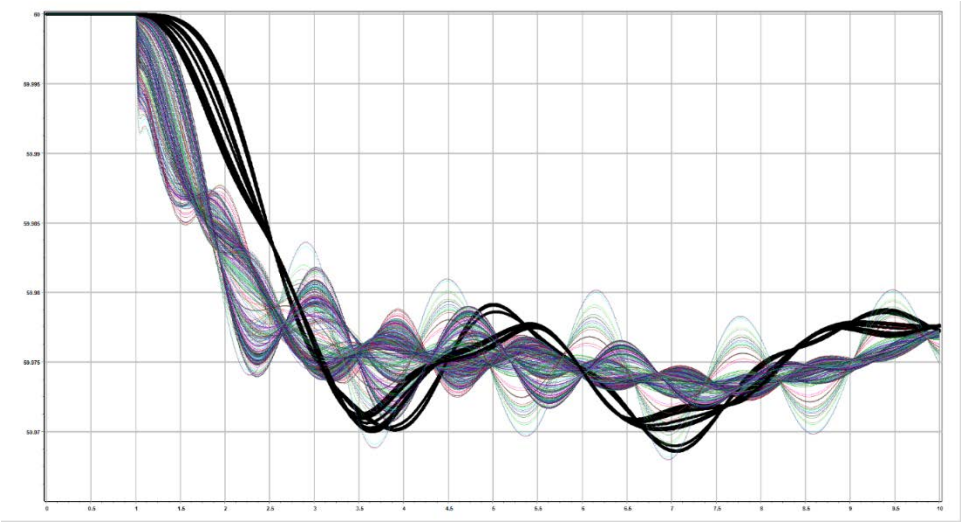

Figure 49. Bus frequency at all buses for a loss of generation (Baltic frequencies are black)

Even by simple visual inspection of the frequency responses given in Figures 48 and 49 it can be seen that the interconnection does have an impact of the overall dynamic behavior of the grid. To further investigate the effect, modal analysis was again conducted, now analyzing the frequency waveforms from entire grid and the results are given in Table 14.

Table 14. Identified modes with Baltics connected

Frequency (Hz)	Damping (%)
0.23	48.9
0.45	8.0
0.62	6.0
0.89	10.2

From the Table 14, it can be seen that there wasn't a large impact to ENTSO-E with the Baltic States connected, which is expected considering the large relative difference in inertia between the two. Figure 50 illustrates this in contouring and Figure 51 shows the quantitative comparison between the two.

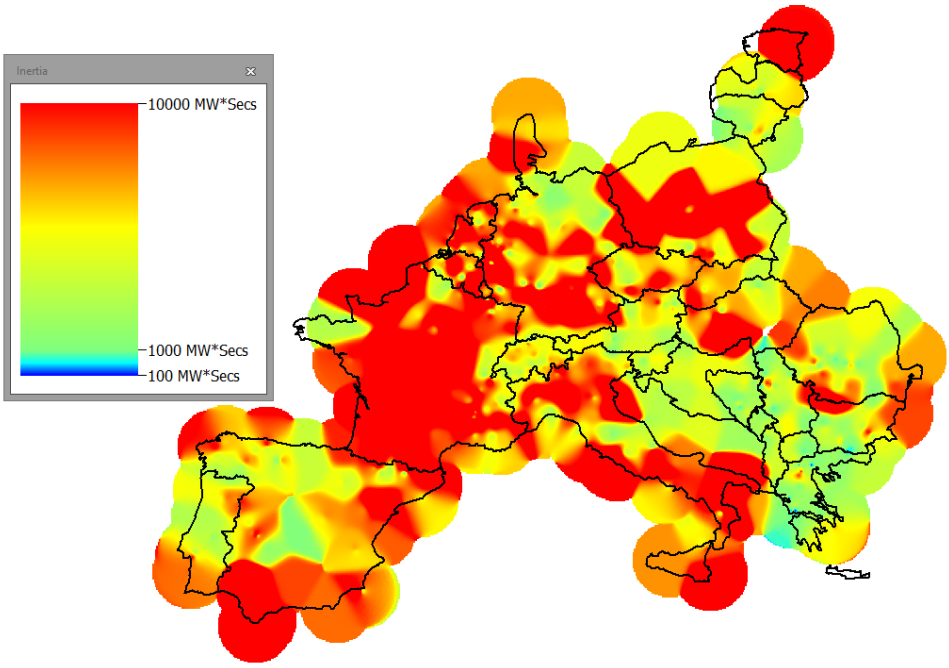

Figure 50. Combined case inertia distribution (MW*secs)

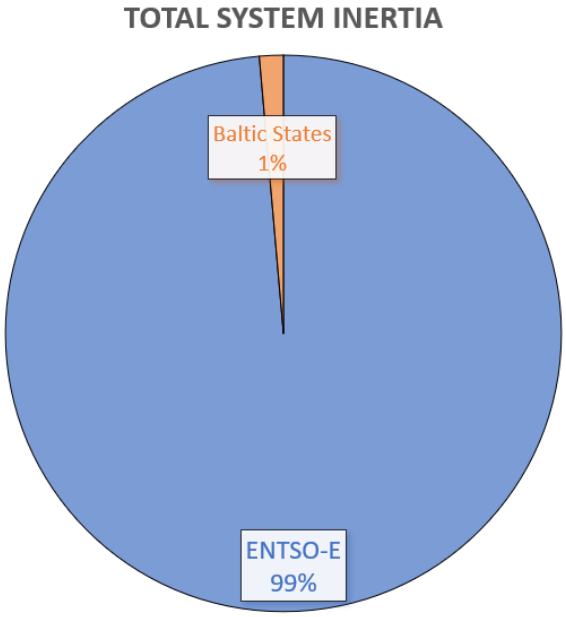

Figure 51. Comparison of case inertia distribution

However, Table 14 shows that there was a slight shift in two modes, and the damping was impacted on one of those. These modes are shown in Figure 52.

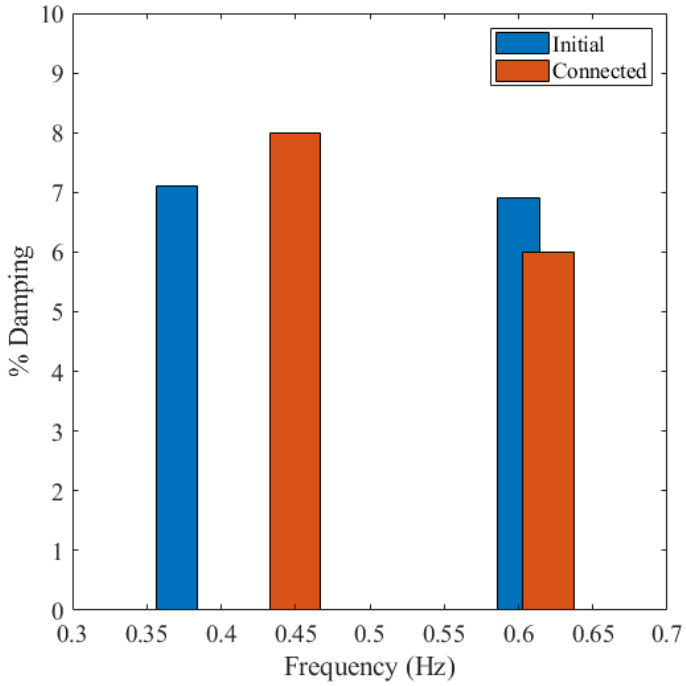

Figure 52. Changes in mode frequency and damping ratios between the two cases

5.3.3. Case 3 – Interconnected Grid – Impact of the Synchronization on the Baltics grid

The impact of Baltic States on the ENTSO-E has been demonstrated, however the resulting impact of the interconnection on the Baltic States is something that needs to be examined in further detail. Here, more detailed studies of the frequency response caused by the generation loss event were conducted. Figure 53 shows the times series of generator bus frequencies in Baltics territory and the larger frequency deviations propagated to the Baltics.

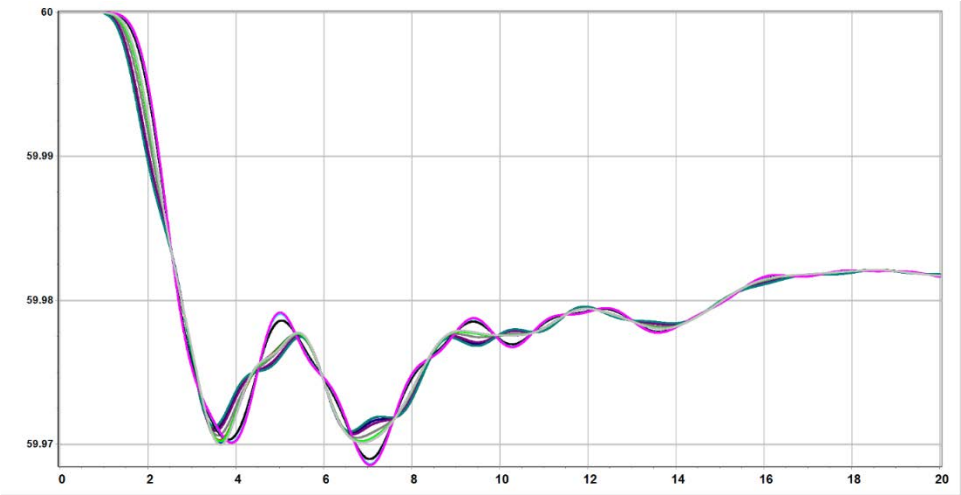

Figure 53. Baltic generator bus frequencies

Through inspection it looks as though the event not only caused a frequency deviation of the entire Baltic grid, but that it also exposed a local oscillation in the Baltic states (this is shown in greater detail in Figure 54. This is a result of the new “islanded” topology of the Baltic grid being disconnected from the IPS/UPS as illustrated in Figure 43.

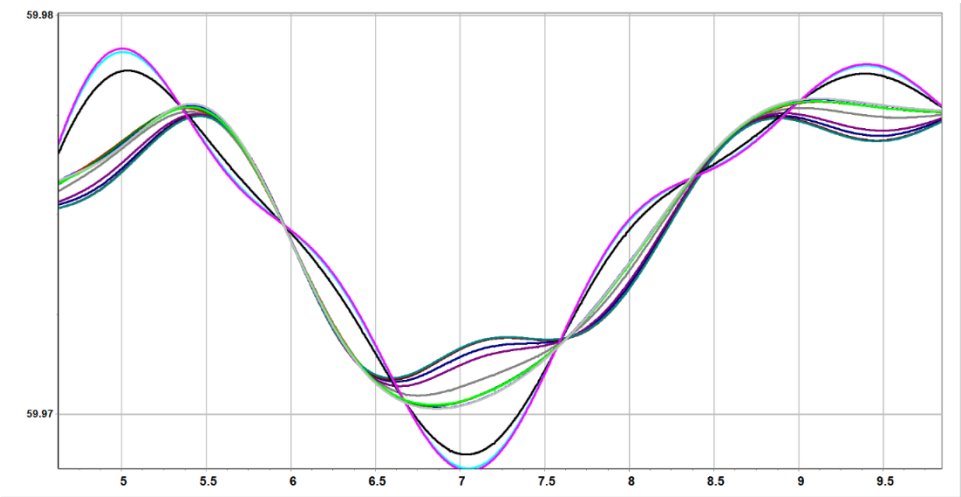

Figure 54. Baltic generator bus frequencies, zoomed to show the presence of a local oscillation

MPM was performed on the signals shown in Figure 54 to examine the oscillatory behavior of the Baltic States, with the results shown in Table 15.

Table 15. Identified modes in Baltic grid only

Frequency (Hz)	Damping (%)
0.26	22.3
0.70	3.28

While mode at the 0.26 Hz does not looks critical, the 0.7 Hz mode has very low damping ratio and requires further attention. Figure 55 shows the frequency contour of the detected mode, with Figure 56 being the power flow between the Baltic states (power transfer largely occurring between Estonia and Lithuania through Latvia).

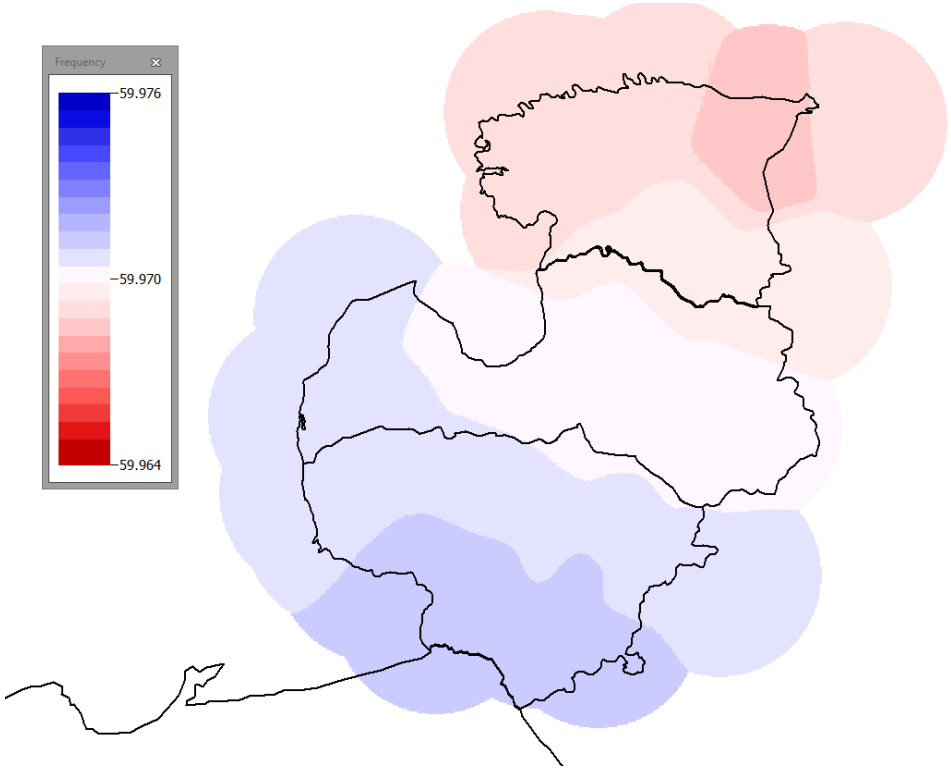

Figure 55. N-S mode of the Baltic States at 0.7 Hz

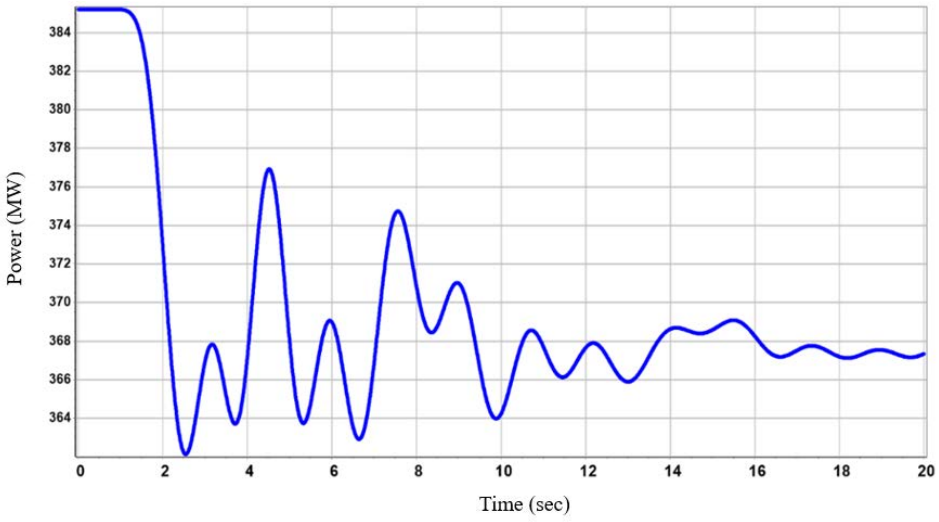

Figure 56. MW flow between north and south Baltic States

Chapter 6: Conclusions and Future Work

6.1. Conclusions

Today, the power system of the Baltic States which includes Lithuania, Latvia, and Estonia, is synchronized with the IPS/UPS. It is planned that by 2025 they desynchronize from the IPS/UPS system and to join the largest interconnection in the world, Continental Europe CE through an HVAC Lithuania-Poland interconnector, in addition to the "soft-coupling" through existing HVDC links.

When initially looking over the planned 2025 transmission configuration, it was likened to a similar situation that exists in WECC (specifically between the Canadian province of Alberta and its electrical connection to the rest of the WECC). The Alberta connection to the WECC has introduced system behavior that can alter how WECC is operated. Likewise, the WECC interconnection introduced new behavior into the Alberta system as well. More specifically, a major event occurring in WECC (such as a generator loss) propagates to the Alberta system, and at the end of the radial tie to the interconnection, it acts as the "tail of a whip." This subsequent impact on Alberta can often lead to disconnection of the grids due to the extreme transient that can occur.

While, the Baltic States -ENTO-E and Alberta - WECC do not match by size, the nature of the connection is still comparable thus, it is worth exploring the impact of the similar events to determine that resulting system events do not have the same level of effect. To help quantify these impacts, a case modeling the entire ENTSO-E and Baltic States was built in this research.

The ENTSO-E DC power-flow case was used as the seed case. This thesis has detailed: 1) the procedure to find an AC solution from this "seed" case; 2) define a methodology for building the transmission system model from scratch using only publicly available data and 3) building the dynamic data necessary for dynamic analysis, some of which were conducted.

The built model of the integrated grid allows a wide range of studies, from steady state to dynamic and it could further help in the development of the new control and protection schemes to assist in increased system stability. To demonstrate the value of the developed model, transient stability analyses were performed on the interconnected model to analyze the impact of the Baltic States on the dynamic stability of the interconnected grid, and the impact of events in the European grid on the Baltic States through the synchronous connection.

The studied topology did not show a significant impact on the ENTSO-E dynamic stability, however the impact on the Baltic grid was detected. Specificity, it has been observed that the loss of a large generator in Continental Europe can excite the new North-South mode between the Baltic States and potentially jeopardize the stability of the grid (damping ratio is quite low). Also, depending on the control and protection schemes that are going to be in place, such events could cause the frequent disconnection of the Baltics from the rest of the systems, as a result reducing the reliability of the grid.

While it is noted that this is a notional reduced-order representation of the ENTSO-E and its connection to the 2025 topology of the Baltic grid, these analyses were performed in understanding that the actual system will behave in a similar manner. Three major takeaways from this work that will be seen in the real-world are: 1) the Baltic's disconnection from the UPS/IPS will result in an oscillatory mode in the Baltic Grid. 2) a major generation loss occurring in ENTSO-E will have an impact the synchronized Baltic grid. 3) connection of the Baltic grid will change the oscillatory behavior of ENTSO-E.

6.2. Future Work

The planned 2025 topology also includes the use of synchronous condensers across the Baltic states in order to increase the short circuit ratio for possible fault conditions. While these are necessary to help support the HVDC interconnects, the inertia that they also provide could negatively impact the overall interactions that the two grids have during transient events. Increased inertia will cause the Baltic grid to become more resistant to changes in frequency, and as such, will cause wider swings during generator loss transients. However, it is also possible to further "tune" the PSS models to increase system damping during a large transient.

The expansion of the developed model to include Norway, Finland, and Sweden will also allow the introduction of advanced HVDC dynamic models (for line commutated and voltage source converters), and some possible control functions that these HVDCs could incorporate to potentially mitigate oscillatory concerns.

Finally, while this model is notional, it is based on work with actual system topology. However, model validation and the necessary adjustment of the system dynamics to compare to the real-world baseline and behavior of ENTSO-E will increase the accuracy of the impacts analyzed in this work.

References

[1] J. D. Glover, M. S. Sarma, and T. Overbye, *Power system analysis & design, 5th Edition SI version*. Cengage Learning, 2012

[2] *Baltic Synchronization*, ENTSO-E, 2016. [Online]. Available: [Accessed July 6, 2020].

[3] A. K. Itkonen, and L. Rietdorf. "Energy security: The synchronization of the Baltic States' electricity networks - European solidarity in action," *European Commission*, June 20, 2019. [Online]. Available: https://ec.europa.eu/commission/presscorner/detail/en/IP_19_3337. [Accessed July 6, 2020]

[4] C. Boechler, "Most Severe Single Contingency (MSSC) Impacts on Alberta Balancing Authority Area Operation Observations and Information Sharing," AESO, June 2015. [Online]. Available: https://www.aeso.ca/assets/Uploads/Most-Severe-Single-Contingency-MSSC-document-for-ARC-June2015.pdf. [Accessed July 6, 2020].

[5] WECC Joint Synchronized Information Subcommittee, "Modes of Inter-Area Power Oscillations in Western Interconnection," November 30, 2013. [Online]. Available: https://www.wecc.org/Reliability/WECC%20JSIS%20Modes%20of%20Inter-Area%20Oscillations-2013-12-REV1.1.pdf. [Accessed July 6, 2020].

[6] A. Muir, and J. Lopatto. "Final report on the August 14, 2003 blackout in the United States and Canada: causes and recommendations." *US–Canada Power System Outage Task Force, Canada*, 2014.

[7] P. W. Sauer, and M. A. Pai, *Power system dynamics and stability*, 1997, Fig 1.2

[8] ABB, "Why HVDC: Economic and Environmental Advantages", https://new.abb.com. [Online]. Available: https://new.abb.com/systems/hvdc/why-hvdc/economic-and-environmental-advantages. [Accessed July 6, 2020].

[9] P. Kundar, *Power System Stability and Control*. New York: McGraw-Hill Companies. 1994.

[10] PowerWorld Corporation, "Transient Stability Overview: Generator Models",. [Online]. Available: https://www.powerworld.com/WebHelp/Default.htm#MainDocumentation_HTML/Transient_Stability_Overview_Generator.htm. [Accessed July 6, 2020].

[11] M. Klein, G. J. Rogers, P. Kundur, "A Fundamental Study of Inter-Area Oscillations in Power Systems," *IEEE Trans. Power Systems*, vol. 6, pp. 914-921, Aug. 1991.

[12] J. Hauer, E. Martinez, A. R. Messina, and J. Sanchez-Gasca. “Identification of Electromechanical Modes in Power Systems.” *Special Publication, TP462, IEEE Power & Energy Society, Tech. Rep.* 2012.

[13] J. D. Follum, F. K. Tuffner, L. A. Dosiek, and J W. Pierre. *Power System Oscillatory Behaviors: Sources, Characteristics, & Analyses*. No. PNNL-26375. Pacific Northwest National Lab. (PNNL), Richland, WA (United States), 2017.

[14] A.R. Borden, B.C. Lesieutre, J. Gronquist “Power system modal analysis tool developed for industry use.” *2013 North American Power Symposium (NAPS)*, Manhattan, KS

[15] T. Becejac, *Synchrophasors: Multilevel Assessment and Data Quality Improvement for Enhanced System Reliability*. PhD diss., 2019. Texas A&M University

[16] *PowerWorld Simulator*. (version 22, 2020). [Online]. Available: https://www.powerworld.com/

[17] PowerWorld Corporation, “Power Flow Analysis and Voltage Control using Simulator,” 2008. [Online]. Available: https://www.powerworld.com/files/TrainingI07VoltageControl.pdf

[18] N. Hutcheon and J. W. Bialek, “Updated and validated power flow model of the main continental European transmission network,” *2013 IEEE Grenoble Conference*, Grenoble, 2013, pp. 1-5, doi: 10.1109/PTC.2013.6652178.

[19] *Europe winter 2009 model:* April 9, 2013. [Online]. Available: https://www.powerworld.com/knowledge-base/updated-and-validated-power-flow-model-of-the-main-continental-european-transmission-network

[20] A. B. Birchfield, *The Creation, Validation, and Application of Synthetic Power Grids*. PhD diss., 2018. Texas A&M University

[21] ARPA-E, “GRID DATA Program,” January 15, 2016. [Online]. Available: https://arpa-e.energy.gov/?q=arpa-e-programs/grid-data.

[22] C. J. Mozina et al., “Coordination of generator protection with generator excitation control and generator capability,” 2009 *62nd Annual Conference for Protective Relay Engineers*, Austin, TX, 2009, pp. 150-164, doi: 10.1109/CPRE.2009.4982510.

[23] R. Schellberg, “Solving Exported GridView Hour,” June 30, 2020. [Online]. Available: https://www.wecc.org/Administrative/Solving%20Exported%20GridView%20Hour_RS.pdf [Accessed July 16, 2020].

[24] A. B. Birchfield, T. Xu and T. J. Overbye, “Power Flow Convergence and Reactive Power Planning in the Creation of Large Synthetic Grids,” in *IEEE Transactions on Power Systems*, vol. 33, no. 6, pp. 6667-6674, Nov. 2018, doi: 10.1109/TPWRS.2018.2813525.

[25] C. Coffin et al, “Approximating Line Losses and Apparent Power in AC Power Flow Linearizations,” Los Alamos National Laboratory technical report: LA-UR-11-06748

[26] *European Union countries – shapefile.* [Online]. Available: https://data.opendatasoft.com/explore/dataset/european-union-countries@public/export/

[27] Interconnected network of ENTSO-E map. [Online]. Available: https://www.entsoe.eu/data/map/downloads/

[28] Population density map. [Online]. Available: https://popdensitymap.ucoz.ru/news/2015-02-18

[29] National electricity demand and generation, Litgrid, Vilnius, Lithuania. [Online]. Available: https://www.litgrid.eu/index.php/power-system/power-system%20information/national-electricity-demand-and-generation/3523

[30] Annual statement of transmission system operator for the year 2015, AST, Riga, Latvia. [Online]. Available: http://www.ast.lv/en/events/annual-statement-transmission-system-operator-year-2015

[31] Electricity consumption and production, Elering AS, Tallinn, Estonia. [Online]. Available: https://elering.ee/en/elektricity-consumption-and-production

[32] Ignitis Gamyba: Electricity Generation [Online] https://ignitisgamyba.lt/en/our-activities/electricity-generation/4186/?c-36/t-72

[33] List of power stations in Latvia [Online]: https://en.wikipedia.org/wiki/List_of_power_stations_in_Latvia

[34] ICIC Power Perspective: Estonia will close 619MW of oil shale generation in 2019. [online] https://www.icis.com/explore/resources/news/2018/09/07/10257649/icis-power-perspective-estonia-will-close-619mw-of-oil-shale-generation-in-2019/?redirect=english

[35] Elering, “Synchronization with continental Europe” [Online]. Available: https://elering.ee/en/synchronization-continental-europe

[36] G. Tcheslabski, “Synchronous machines: Construction of synchronous machines”, 2016. [Online]. Available: ee.lamar.edu/gleb/teaching.html

[37] Y.V. Makarov, M.A. Elizondo, J.G. O'Brien, Q. Huang, H. Kirkham, Z. Huang, M. Chinthavali, D. Suman, N. Mohan, W. Hess, and D. Duebner, 2017. *Models and methods for assessing the value of HVDC and MVDC technologies in modern power grids*. (No. PNNL-26640). Pacific Northwest National Lab. (PNNL), Richland, WA (United States).